Cell

Drosophila Cytokine Unpaired 2 Regulates Physiological Homeostasis by Remotely Controlling Insulin Secretion

Akhila Rajan[1,*] and Norbert Perrimon[1,2,*]
[1]Department of Genetics
[2]Howard Hughes Medical Institute
Harvard Medical School, 77 Avenue Louis Pasteur, Boston, MA 02115, USA
*Correspondence: akhila@genetics.med.harvard.edu (A.R.), perrimon@receptor.med.harvard.edu (N.P.)
http://dx.doi.org/10.1016/j.cell.2012.08.019

SUMMARY

In *Drosophila*, the fat body (FB), a functional analog of the vertebrate adipose tissue, is the nutrient sensor that conveys the nutrient status to the insulin-producing cells (IPCs) in the fly brain to release *Drosophila* insulin-like peptides (Dilps). Dilp secretion in turn regulates energy balance and promotes systemic growth. We identify Unpaired 2 (Upd2), a protein with similarities to type I cytokines, as a secreted factor produced by the FB in the fed state. When *upd2* function is perturbed specifically in the FB, it results in a systemic reduction in growth and alters energy metabolism. Upd2 activates JAK/STAT signaling in a population of GABAergic neurons that project onto the IPCs. This activation relieves the inhibitory tone of the GABAergic neurons on the IPCs, resulting in the secretion of Dilps. Strikingly, we find that human Leptin can rescue the *upd2* mutant phenotypes, suggesting that Upd2 is the functional homolog of Leptin.

INTRODUCTION

Integration of information regarding nutrient status with other physiological processes, such as systemic growth, energy expenditure, feeding, and reproduction, is a complex function performed by multicellular organisms. Disruption of this fundamental homeostatic process can lead to a number of disorders, in particular obesity, anorexia, and diabetes (Morton et al., 2006). In addition, it can have profound effects on cancer and aging (Hursting et al., 2003).

Insulin peptides are key hormones involved in the regulation of carbohydrate and lipid metabolism, tissue growth, and longevity (Taguchi and White, 2008). Circulating insulin absorbs nutrients such as glucose and lipids, and stores them for later use in the form of glycogen and triacylglycerol (TAG). When insulin production from pancreatic beta cells is disrupted in mammals, as in the case of Type I diabetes, the body is unable to utilize the nutrients consumed and instead mounts a starvation response whereby stored lipids and glycogen are broken down to generate energy (Kahn et al., 2005). The production of insulin by pancreatic beta cells is tightly regulated to ensure that appropriate amounts are released into the blood depending on nutrient status and food intake.

The insulin pathway is highly conserved from mammals to *Drosophila* and serves fundamentally the same physiological functions (Taguchi and White, 2008; Wu and Brown, 2006). A main difference, however, is that the fly insulin-producing cells (IPCs), which are homologous to pancreatic beta cells, are found in the brain (Rulifson et al., 2002). These IPCs lie in the brain median neurosecretory cluster (mNSC) and produce at least three of the eight known *Drosophila* insulin-like peptides (Dilp2, Dilp3, and Dilp5) (Brogiolo et al., 2001; Ikeya et al., 2002). A deficiency that uncovers multiple Dilps (*Dilp1–Dilp5*) results in flies that, in addition to being smaller, have decreased TAG and increased circulating sugars (Kulkarni et al., 1997). Dilps secreted from the IPCs bind to the insulin receptor in peripheral tissues to promote growth and nutrient utilization.

The fat body (FB) functions as a key sensor of the nutritional status of the fly and couples systemic growth, metabolism, and stem cell maintenance with nutritional availability. Studies using ex vivo organ cocultures of FBs and larval brains proposed that the FB secretes growth-promoting factors (Britton and Edgar, 1998; Davis and Shearn, 1977). Suppression of amino acid (AA) transport in the FB by knocking down the AA transporter *slimfast* (*slif*) resulted in flies with systemic growth defects, suggesting that the FB acts as a nutrient sensor that nonautonomously modulates insulin signaling based on nutrient status (Colombani et al., 2003; Géminard et al., 2009). When flies were cultured on rich food, the amount of Dilp accumulation was considerably lower in the IPCs compared with the level of Dilps in IPCs of nutrient-deprived flies. Consistent with this, the level of Dilps in the hemolymph of fed flies was higher than in starved flies (Géminard et al., 2009). Altogether, these results suggest that the regulation of organismal growth in response to nutrient availability involves the control of insulin secretion from brain IPCs by factors originating from the FB.

Here, we identify Unpaired 2 (Upd2), a *Drosophila* cytokine, as a secreted factor produced by the FB in response to dietary fat and sugars. Upd2 activates Janus kinase (JAK)/Signal Transducer and Activator of Transcription (STAT) signaling in

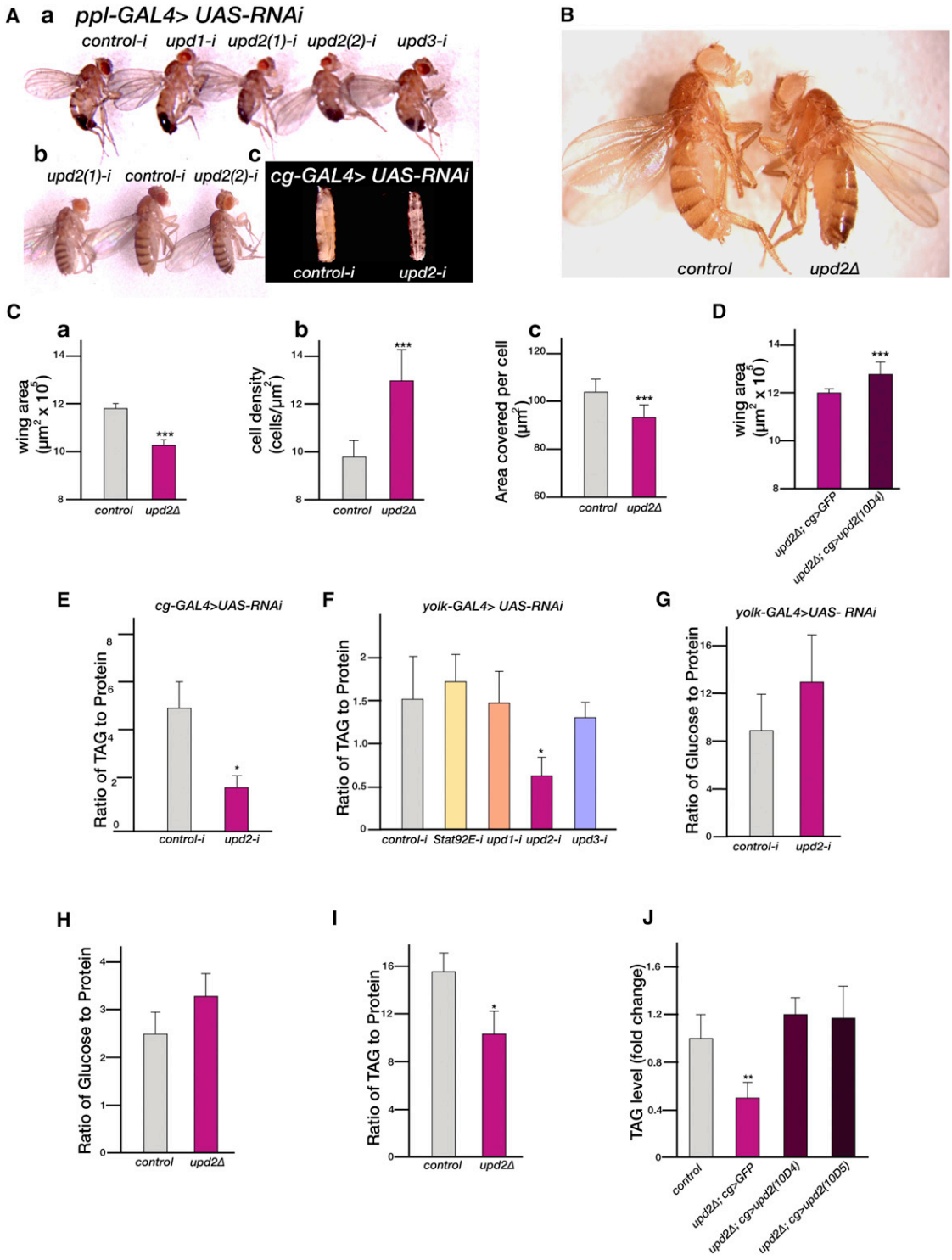

Figure 1. Upd2 Controls Systemic Growth and Metabolism

(A) Adult flies with FB-specific knockdown of *upd1*, *upd2*, and *upd3* using the *ppl-GAL4* driver (*ppl-GAL4* > *upd-RNAi*, subpanel a). RNAi of *upd2* (*upd2-RNAi*, indicated as *upd2-i* in the figure) using two independent lines (lines 1 and 2) results in size reduction of both adult males (subpanel a) and females (subpanel b). Note that in the subsequent figures, because *upd2(1)-i* and *upd2(2)-i* gave the same results, we used the *upd2(1)-i* line and simply refer to it as *upd2-i*. *cg-GAL4* > *upd2-RNAi* third instar larvae are smaller and slimmer than control (subpanel c). Control-i is *Luciferase-RNAi*.

(B) Hemizygous adult males for the *upd2* deletion allele (*upd2Δ*) appear smaller and slimmer than the *y w* controls.

(C) Quantification of the wing area (subpanel a), cell size (subpanel b), and cell density (subpanel c) of *upd2Δ* males compared with *y w* control.

GABAergic neurons, relieving their inhibitory effect on the IPCs and in turn resulting in the secretion of Dilps into the hemolymph to promote systemic growth and fat storage. The similarities between Upd2 and vertebrate Leptin are striking because Leptin is secreted from the adipose tissue in mammals under conditions of nutritional surplus, and high fat levels in particular (Zhang et al., 1994). We show that human Leptin can functionally substitute for *Drosophila* Upd2 and can function as a ligand to the JAK/STAT receptor Dome *Drosophila*. Altogether, our studies illustrate how a cytokine-mediated pathway regulates the secretion of insulin to modulate systemic growth according to nutrient availability, in particular dietary fats, and provides evidence for the evolutionary conservation of this signaling module.

RESULTS

Upd2 Plays an FB-Specific Role to Control Systemic Growth

Cytokines are secreted molecules that communicate intercellular signals and thus are ideal candidates for remotely signaling nutritional status (Dinarello and Mier, 1986) and signal through the JAK/STAT pathway. In the *Drosophila* genome, three related Upd ligands—Upd1, Upd, and Upd3—have predicted secondary structures similar to that of type I cytokines (Boulay et al., 2003) and regulate the activity of the JAK/STAT pathway (Wright et al., 2011; Zeidler et al., 2000). They bind to the transmembrane receptor Domeless (Dome) (Brown et al., 2001), which in turn activates the JAK Hopscotch (Hop) (Binari and Perrimon, 1994). Activated Hop regulates STAT92E/Marelle (Hou et al., 1996). Because cytokines play central roles in mammalian nutrition sensing and metabolic homeostasis, we reasoned that their fly counterparts could be involved in similar processes.

To investigate the role of the Upd cytokines in the FB, and their effects on overall body size, we used RNA interference (RNAi) to knock down their expression. At least two independent RNAi lines per gene and two different FB GAL4 drivers (*ppl-GAL4;* and *cg-GAL4*) were used to ensure that the knockdown was both gene and tissue specific. The efficiency of knockdown of all three genes in the larval FB was comparable (*upd1*, 80%; *upd2*, 60%; and *upd3*, 70%) as analyzed by quantitative PCR (qPCR). Of interest, only FB-specific knockdown of *upd2*, and not *upd1* or *upd3*, resulted in smaller flies (Figures 1Aa and 1Ab) and larvae (Figure 1Ac), suggesting that this ligand alone plays an FB-specific role in regulating systemic growth. In further support of the model that the effect of Upd2 on systemic growth is specific to the FB, knockdown of *upd2* specifically in larval muscles did not affect body size (Figures S1A and S1B available online).

Previously, an *upd2* homozygous deletion mutant (*upd2Δ*) that removes the 5′UTR and the first 89 AAs was identified and reported to be viable and fertile (Hombría et al., 2005). An examination of the growth phenotypes of *upd2Δ* flies, compared with an age- and population-density-matched control, showed that the *upd2Δ* flies were significantly slimmer and smaller (Figure 1B), similar to the phenotype generated with FB-specific knockdown of *upd2Δ* (Figure 1Ab). An examination of the wings, a tissue that can be easily quantified for growth phenotypes, revealed that *upd2* mutant wings have a 10% reduction in overall size (Figure 1Ca) and a significant reduction in both cell number (Figure 1Cb) and cell size (Figure 1Cc). Expression of an *upd2* cDNA in the FB of *upd2Δ* flies was able to rescue the wing size phenotype (Figure 1D), providing further evidence that *upd2* plays an FB-specific role in the regulation of systemic growth.

Upd2 Plays an FB-Specific Role to Control Metabolism

To test whether Upd2 plays a role in regulating energy metabolism, we measured the levels of triacylglycerol (TAG) in larvae with FB-specific knockdown of *upd2*. TAG levels were significantly reduced (Figure 1E). Similarly, *upd2Δ* larvae also showed a significant reduction in TAG levels (data not shown). Knockdown of *upd2* specifically in other tissues, such as larval muscles, did not affect stored fat levels or body size (Figure S1), consistent with the model that the function of Upd2 is specific to the FB.

In *Drosophila*, organismal growth is restricted to larval stages, and genetic manipulations that affect nutrient sensing during adulthood lead to metabolic phenotypes. To assay whether Upd2 plays a specific role in nutrient sensing in adults, we used a GAL4 driver that is expressed only in the adult FB (*yolk-GAL4*; see Experimental Procedures) and measured TAG levels in flies 15 days after eclosion. FB-specific knockdown of *upd2* (Figure 1G) was associated with an increase in the amount of circulating sugar in the hemolymph, suggesting that Upd2 plays a role in the FB to regulate overall energy metabolism. Consistently, *upd2Δ* adults displayed an increase in the levels of circulating sugars (Figure 1H), and a significant reduction in TAG levels (Figure 1I) that could be rescued by expressing an *upd2-cDNA* in the FB (Figure 1J). Of interest, knockdown of *stat92E*, the transcription factor that mediates JAK/STAT pathway activity, in the FB (efficiency of knockdown in the FB as assayed by qPCR > 90%) did not affect TAG storage (Figure 1F), indicating that Upd2 plays a nonautonomous role in regulating fat storage.

Altogether, these results indicate that Upd2 in the FB regulates systemic growth in larvae and energy metabolism in both larvae and adults. Further, the effect of Upd2 is likely FB

(D) Rescue of the wing area phenotype of *upd2Δ* males by FB-specific expression of *upd2* cDNA using *cg-GAL4*.
(E) Quantification of TAG to protein in male larvae with FB-specific knockdown of *upd2* using *cg-GAL4*.
(F) Ratio of TAG to protein in adult females with FB-specific knockdown of JAK/STAT pathway components using *yolk-GAL4*.
(G) Circulating sugars in the hemolymph of female adults with FB-specific knockdown of *upd2*. In (E)–(G) the control is *white-RNAi*.
(H) Ratio of glucose to protein in the hemolymph of *upd2Δ* adult males compared with *y w* controls.
(I) Ratio of TAG to protein in adult *upd2Δ* males compared with *y w* controls.
(J) Rescue of the TAG phenotype in *upd2Δ* adult males with FB-specific expression of either 10D4 or 10D5 *upd2* cDNA using *cg-GAL4*. Error bars in the figures represent the standard deviation (SD); p values were calculated using Welch's t test (*p < 0.05, **p << 0.01, ***p << 0.00001).
See also Figure S1.

nonautonomous, as removal of *stat92E* from the FB is not associated with an effect on systemic growth.

Upd2 Signals the Fed State and Senses Fat and Sugars

To explore the relationship between Upd2 expression in the FB and the nutritional state, we examined *upd2* transcript levels under starvation. Strikingly, we found that *upd2* transcripts showed a 98% reduction (Figure 2A) in adult wild-type males that were starved on 1% sucrose agar for >72 hr. Because a reduction in size and energy metabolism could result from reduced nutritional intake, we measured fly feeding using both blue dye (Xu et al., 2008) and capillary feeder (CAFÉ) assays (Ja et al., 2007). Both tests, performed in three to five replicates on age- and population-density-matched adult male flies, showed that neither the FB-specific knockdown of *upd2* nor the *upd2Δ* flies had feeding-behavior defects (Figures 2B and 2C).

To assess whether *upd2* senses the nutritional state of the organism, we analyzed lipid storage in hepatocyte-like cells/oenocytes that accumulate lipid droplets only under conditions of nutritional deprivation and not under a fed state (Gutierrez et al., 2007). Whereas the control larvae did not accumulate lipid droplets under fed conditions (Figure 2D), *upd2Δ* larvae showed a striking accumulation of lipid droplets in oenocytes, as assayed by Oil Red O staining, even under conditions of nutritional surplus (Figure 2D). Because *upd2Δ* flies feed normally, this lipid accumulation suggests that Upd2 is required to sense the appropriate nutritional state.

Given that knocking down the AA transporter *slif* mimics the starvation state (Colombani et al., 2003; Gutierrez et al., 2007), we examined the *upd2* steady-state mRNA levels in FB-specific *slif* knockdown (*ppl-GAL4 > UAS-slif^{anti}*) by qPCR. Strikingly, the *upd2* level increased by >2-fold, whereas another JAK/STAT ligand, *upd1*, and the downstream component *STAT92E* were not significantly altered (Figure 2E). Slif plays a role in transporting AAs, and its absence results in a protein-deprived state. Hence, the upregulation of *upd2* under this state (Figure 2E) suggests that the upstream signal for *upd2* expression is not nutrition-derived proteins.

We next assayed *upd2* expression in adult male flies subjected to diets rich in protein, fat, or sugar, and compared *upd2* mRNA levels under these conditions with respect to standard lab food. In many independent experiments, we consistently found that 5 days after exposure to high-fat and high-sugar diets, the normalized steady-state level of *upd2* mRNAs went up by 4- to 6-fold, a statistically significant difference compared with levels obtained on standard lab food (Figure 2F). Taken together, these results strongly argue that *upd2* senses the fed state downstream of fats and sugars.

To address whether Upd2 is sufficient to signal the fed state, we tested whether overexpression of *upd2* in wild-type flies can suppress the starvation response associated with nutrient deprivation. We measured the breakdown of stored fat in starved flies overexpressing *upd2* in the FB using thin-layer chromatography (TLC). TLC was performed on adult flies to measure the fat stores after a period of 24 hr on 1% agar. Whereas in control flies the stored fat levels were nearly depleted after 24 hr (Figure 2G; 98% reduction), the reduction was not significant in flies overexpressing *upd2* in their FB (Figure 2G; 35% reduction). Thus, Upd2 can suppress stored fat breakdown under conditions of starvation, indicating that it signals a fed condition even when flies are deprived of nutrients.

Brain IPCs secrete Dilps in response to nutrition and accumulate Dilps under conditions of nutrient deprivation (Géminard et al., 2009). To test whether Upd2 overexpression in the FB can suppress accumulation of Dilps in the IPCs under conditions of starvation, age- and population-density-matched adult flies overexpressing Upd2 in the FB were starved for 24 hr on 1% agar. We then dissected and stained the brains for Dilp2 and Dilp5, analyzed them by confocal microscopy, and calculated the mean Dilp fluorescence. Strikingly, Dilp2 and Dilp5 accumulation was significantly lower in brains of starved flies overexpressing Upd2 in their FB (Figure 2H, 78% less Dilp2; data not shown for Dilp5), revealing that Upd2 expression in the FB alters Dilp2 and Dilp5 accumulation in brain IPCs in response to the nutritional state. Note that in the experiments described below, the same results were observed for both Dilp2 and Dilp5. For simplicity, only the Dilp2 data are shown, and in the text Dilp2 and Dilp5 are referred to as Dilp(s).

The *upd2Δ* mutants and FB knockdown of *upd2* resemble the *dilp1–dilp5* deletion flies with respect to their size and metabolic phenotypes. Hence, we tested whether the primary role of Upd2 is to signal the fed state to the IPCs. Two different FB-specific drivers, *cg-GAL4* (Figure 3A) and *ppl-GAL4* (data not shown), were used for these experiments. RNAi against *upd2* in the FB resulted in a statistically significant increase in mean Dilp fluorescence in larval brains (Figure 3A). This increase in Dilp accumulation was most apparent when the larvae were actively feeding. We performed a qPCR analysis of Dilp in the brains of larvae with FB-specific knockdown of *upd2* RNAi to ensure that the increase in mean Dilp fluorescence was not a result of increased transcription. No significant change in Dilp transcription was observed (Figure S2). In addition, FB-specific knockdown of either *stat92E* or *upd1* did not result in increased accumulation of Dilp (Figure 3A), which is consistent with our observations regarding body size and metabolism (Figure 1). Further, the increase in Dilp accumulation in the IPCs was also observed in both larval (data not shown) and adult *upd2Δ* homozygous mutant brains (Figure 3B). Finally, the accumulation of Dilp in the IPCs of *upd2Δ* homozygous mutants could be rescued by expressing *upd2* cDNA in the FB (Figure 3Bc), indicating that the inability to release Dilps underlies both the systemic growth and energy metabolism phenotypes of *upd2Δ* mutants.

IPCs in the *Drosophila* brain use membrane voltage-dependent neurosecretory mechanisms to facilitate Dilp release in response to nutrition (Géminard et al., 2009). Thus, if Upd2 promotes Dilp secretion under fed conditions, activating Dilp secretion in *upd2Δ* homozygous mutants should rescue the *upd2Δ* growth phenotype. To achieve this, we depolarized the IPCs by expressing the bacterial sodium channel (NaChBac) (Luan et al., 2006; Ren et al., 2001) under the control of the *Dilp3-GAL4* driver, which drives expression specifically in the brain IPCs during both larval and adult stages. Under these conditions, the level of Dilp accumulation in the IPCs of *upd2Δ* was significantly reduced (Figure 3C). In addition, this artificial depolarization of the IPCs in an *upd2Δ* homozygous mutant background rescued the small size of *upd2Δ* mutants

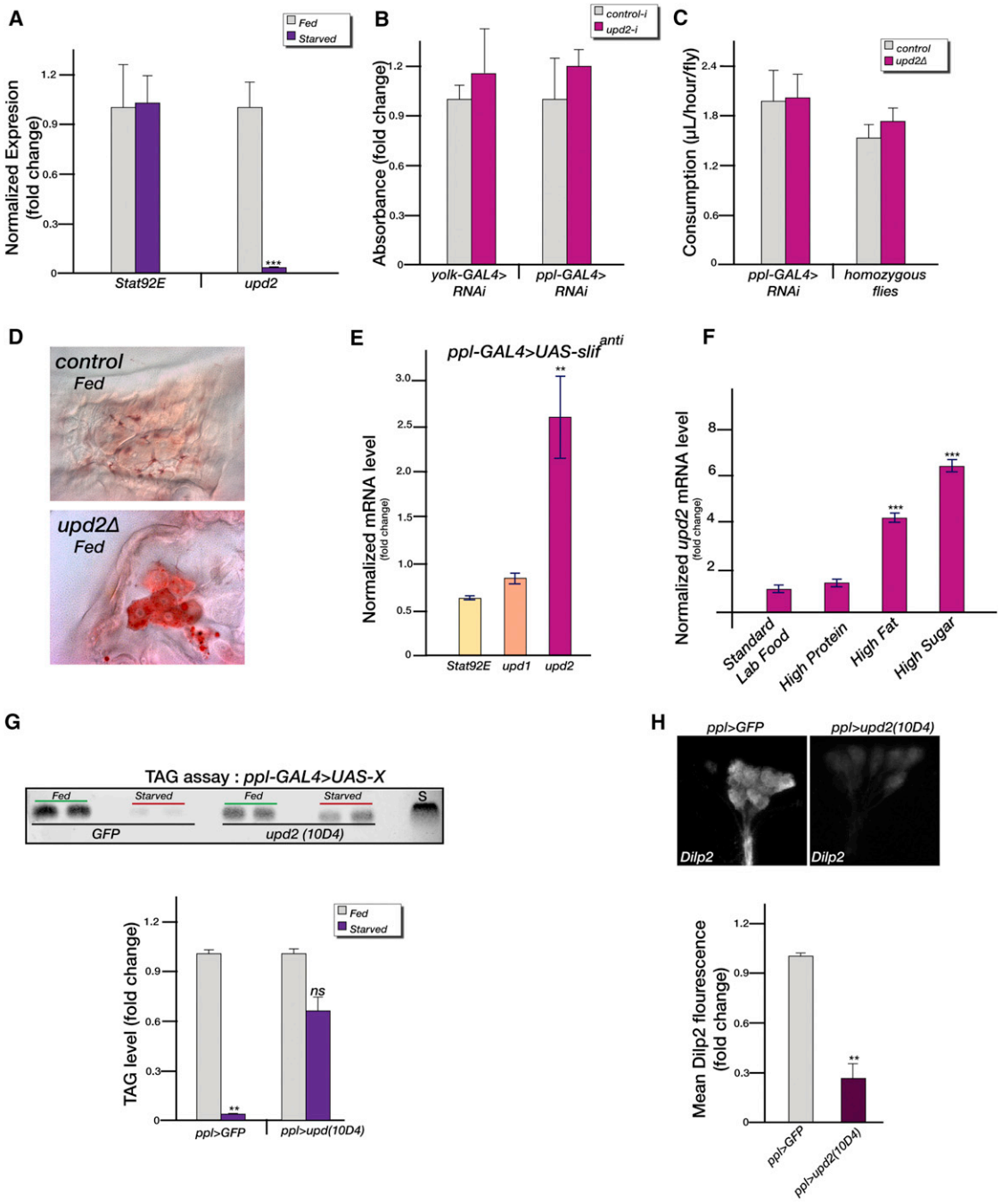

Figure 2. Upd2 Expression in the FB Signals the Fed State

(A) The steady-state mRNA expression of *STAT92E* and *upd2* was analyzed by qPCR.

(B) Blue dye feeding assay in adult males with FB-specific knockdown of *upd2*.

(C) CAFÉ assay in adult males with FB-specific knockdown of *upd2* or *upd2Δ*.

(D) Oil Red O staining of oenocytes in third instar male larvae shows that *upd2Δ* animals accumulate more Oil Red O droplets under fed conditions compared with *y w* controls.

(E) Steady-state mRNA levels in adult males with FB-specific knockdown of *slif* compared with control (*UAS-slif*^{anti}).

(F) qPCR performed on RNA extracted 5 days after adult males were exposed to different diets. The normalized expression level of *upd2* is shown.

(G) TLC was used to assay the amount of stored TAG in adult male flies under fed and starved conditions. TAG was extracted from *ppl-GAL4 > 10D4 upd2-cDNA* or *GFP* (control) adult males. S indicates the mobility of coconut oil used as a marker in the TLC plate.

(H) Dilp2 immunostaining in the IPCs of starved adult male flies expressing *GFP* (control) or 10D4 *upd2-cDNA* using *ppl-GAL4*. Black error bars represent the SD. Blue error bars represent the standard error of the mean; p values were calculated using Welch's t test (*p < 0.05, **p << 0.01, ***p << 0.00001).

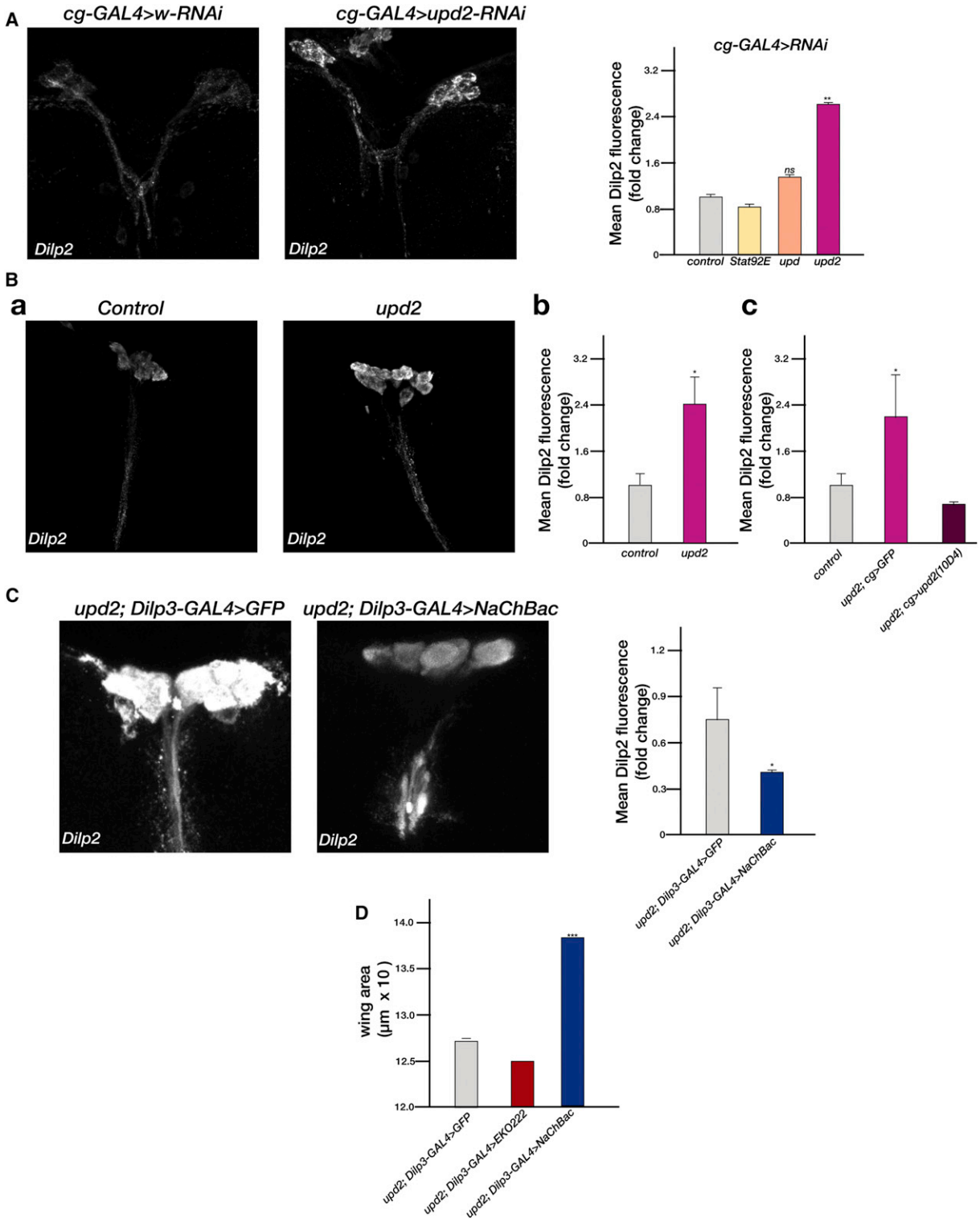

Figure 3. Upd2 Remotely Controls Dilp Accumulation in IPCs

(A) Maximum intensity XY projection (MIP) of *cg-GAL4* male larval brains stained with Dilp2 driving the expression of either *white-RNAi* (control) or *upd2-RNAi*, and quantification of the mean Dilp2 immunofluorescence in larval brains of *cg-GAL4* animals driving RNAi of JAK/STAT pathway components.

(B) MIP of adult male brains stained with Dilp2. The brains were dissected from age-matched *upd2Δ* and *y w* control (subpanel a). A significant increase in Dilp2 fluorescence is observed in *upd2Δ* male brains compared with *y w* (subpanel b). In subpanel c, rescue of Dilp2 accumulation in *upd2Δ* flies by FB-specific expression of the 10D4 *upd2* cDNA using *cg-GAL4*. Brains from *cg-Gal4* flies were used as positive controls (gray bar).

(Figure 3D). Of interest, hyperpolarizing the neurons by expressing the potassium channel rectifier EKO (White et al., 2001) did not exacerbate the *upd2Δ* size phenotype (Figure 3D), indicating that in the absence of *upd2*, the IPC neurons are already depolarized.

In summary, the reduction in TAG levels, increase in circulating sugars, and systemic reduction in body size in the absence of *upd2* resemble a reduction in insulin signaling, suggesting that the primary role of Upd2 is to remotely control the secretion of Dilps from the IPCs in response to nutrient intake.

A STAT Reporter Is Expressed near the IPCs and Is Altered in Response to Starvation

To elucidate how Upd2 regulates Dilp secretion in response to nutrition, we examined the activity of a STAT reporter (10XSTAT::GFP; see Experimental Procedures) that was previously shown to recapitulate JAK/STAT pathway activation (Bach et al., 2007) in the adult brain. We found that STAT::GFP is widely expressed throughout the adult brain in both neurons and glia (Figure S3), and more specifically, it is expressed in the olfactory lobe (Figure 4A, asterisk), the optic lobe (Figure 4A, hash), and the mNSCs (a region that includes the IPCs plus other neurons; see arrow in Figure 4A) of the adult brain. Of importance, an analysis of single optical sections revealed that the STAT reporter is expressed in neurons juxtaposed to the IPCs (arrow, Figure 4B) in the mNSC region of the adult brain and in the larval brain (Figure S4).

Next, we addressed whether the expression of the STAT reporter is altered in response to nutritional deprivation. Under fed conditions, the STAT reporter is expressed in the cell body of neurons immediately adjacent to the Dilp-expressing IPCs (Figure 4C, red arrow). In addition, the STAT reporter is expressed along the neurites that run parallel to the median arborizations of the IPCs (Figure 4C, yellow arrow). Along the neurites, the reporter is enriched in vesicular structures that colocalize with the presynaptic marker Synapsin (Klagges et al., 1996; Figure S5), suggesting that they may correspond to the sites of synaptic contact with the IPCs. Following nutrient deprivation (adult males kept on 1% sucrose agar at 25°C for >72 hr), STAT reporter expression in neurons juxtaposed with the IPCs is altered, and both the expression in the cell body (Figure 4D, red arrow) and the vesicular enrichment along the median branches of the IPCs is reduced or lost (Figure 4D, yellow arrow). Altogether, the alterations in reporter activity in these neurons in response to the nutrient status suggest that they influence Dilp secretion in the fed condition.

If Upd2 controls Dilp levels in the IPCs by activating STAT signaling in the mNSC neurons, then compromising *upd2* function should phenocopy the effect of starvation on STAT reporter expression. We analyzed STAT reporter expression in the adult brains of flies that express *upd2-RNAi* in the FB and compared it with a *luciferase-RNAi* control. Indeed, although the expression of the STAT reporter in the controls was very similar to that observed in the fed condition (Figure 4E), both the expression of the reporter in the cell body (red arrow, Figure 4F) and the vesicular enrichment along the IPCs (Figure 4F, yellow arrow) were much reduced or lost when *upd2* was knocked down in the FB, as observed under starvation.

STAT Signaling in mNSC Neurons Regulates Systemic Growth and Metabolism

To further test the model that JAK/STAT signaling plays a role in the mNSCs to regulate systemic growth and metabolism, we assayed whether knocking down STAT92E in mNSC neurons would affect systemic growth and fat storage. To knock down STAT92E, we used *dome-GAL4* (Mandal et al., 2007), which we found drives expression in a number of neurons in the adult brain, including STAT-reporter-positive mNSCs (Figure 5A, white arrow). At 25°C, *dome-GAL4 > stat92E-RNAi* results in lethality, presumably because of the role of STAT92E in development. However, when cultured at 18°C, the flies emerged but were significantly smaller than the controls (Figure 5B). We shifted *dome-GAL4 > stat92E-RNAi* adults to 29°C for 7 days to allow for a more significant knockdown of STAT92E expression, and assayed for stored fat by performing a TLC assay. Strikingly, the level of stored fat was significantly lower in flies with compromised STAT92E function (Figure 5C). A similar experiment performed with *upd2-RNAi* flies failed to reveal a role for Upd2 in the *dome-GAL4* neurons, as there was no effect on stored fat (Figure 5C) or body size (data not shown).

To examine whether compromising the function of the receiving end of the JAK/STAT pathway results in increased Dilp accumulation in the IPCs, we used *dome-GAL4; tub-GAL80^{ts}* to express *stat92E-RNAi* or *dome-RNAi* only during adulthood (see Experimental Procedures). We assayed the expression of Dilp2 in the IPCs of these flies 7 days after transfer at the restrictive temperature and compared it with a *GFP-RNAi* control. Dilp2 accumulation significantly increased when *stat92E* or *dome* function was compromised in adults (Figure 5D), suggesting that the JAK/STAT pathway plays a role in promoting Dilp2 secretion from the IPCs.

The *dome-GAL4* driver is expressed not only in the brain but also in other tissues of the fly (e.g., gut and muscle). Hence, to address whether JAK/STAT signaling in the mNSC neurons activates/depolarizes or inhibits/hyperpolarizes neuronal activity, we expressed the bacterial sodium channel (NaChBac) using *dome-GAL4* at the restrictive temperature (*dome-GAL4; tub-GAL80^{ts} > NaChBac*). This forced depolarization resulted in reduced fat storage (Figure 5E) and increased Dilp2 accumulation (Figure 5F), suggesting that activation of the JAK/STAT pathway in mNSC neurons prevents their neuronal firing.

JAK/STAT Plays a Role in Neurons Expressing Vesicular GABA Transporter to Modulate Systemic Growth and Metabolism

IPCs express receptors for serotonin and GABA, and both of these neurotransmitters exert an inhibitory effect to prevent

(C) Expression of *NaChBac* in the IPCs of *upd2Δ* adult male brains using *Dilp3-GAL4* significantly reduces Dilp2 accumulation in the IPCs.
(D) Expression of *NaChBac* in the IPCs of *upd2Δ* adult male brains using *Dilp3-GAL4* significantly increases the wing area of *upd2Δ*. Note that further inhibition of neuronal activity using the inward rectifying potassium channel (*EKO222*) does not reduce the wing area any more than removal of *upd2* alone.
Error bars represent the SD; p values were obtained with Welch's t test (*$p < 0.05$, **$p << 0.01$, ***$p << 0.00001$). ns, not significant. See also Figure S2.

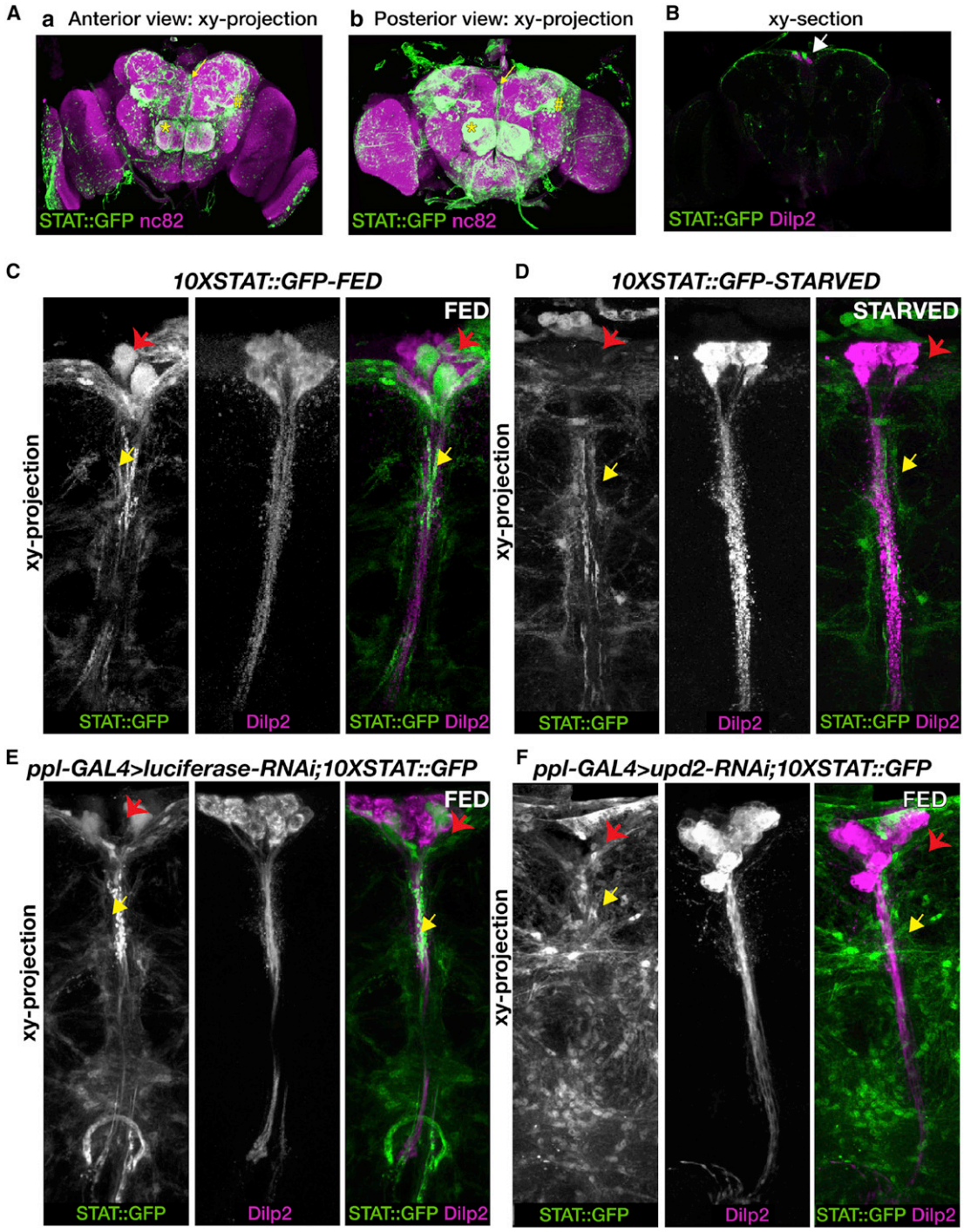

Figure 4. STAT Reporter Expression in the Adult Brain and its Response to Starvation

(A) Anterior (subpanel a) and posterior (subpanel b) MIPs of adult male brains expressing the *10XSTAT::GFP* reporter. nc82 (magenta), a presynaptic active-zone protein marker, identifies the neuropils. *STAT::GFP* (green) is widely expressed, including in the olfactory lobe (asterisk), optic lobe (hash), and mNSCs (arrow).

(B) Single optical section along the XY axis of an adult male brain immunostained for Dilp2 (magenta) and *STAT::GFP* (green). Note that the cell bodies of the STAT reporter-expressing neurons are located right next to the Dilp2-expressing IPCs (arrow points to the juxtaposition of these neurons).

(C–F) Three-dimensional projections along the XY axis of adult male brains stained for Dilp2 (magenta) and *STAT::GFP* (green).

(C) Under fed conditions, the *STAT::GFP* reporter is expressed in neurons immediately adjacent to the Dilp2-expressing IPCs (red arrow). The STAT reporter is expressed along the neurites that run parallel to the median arborizations of the IPCs (yellow arrow).

(D) Under starved conditions, the GFP reporter expression is reduced in the cell body (red arrow) and along the neurites (yellow arrow). Dilp2 fluorescence in the IPCs is increased under starved conditions (D) compared with fed conditions (C).

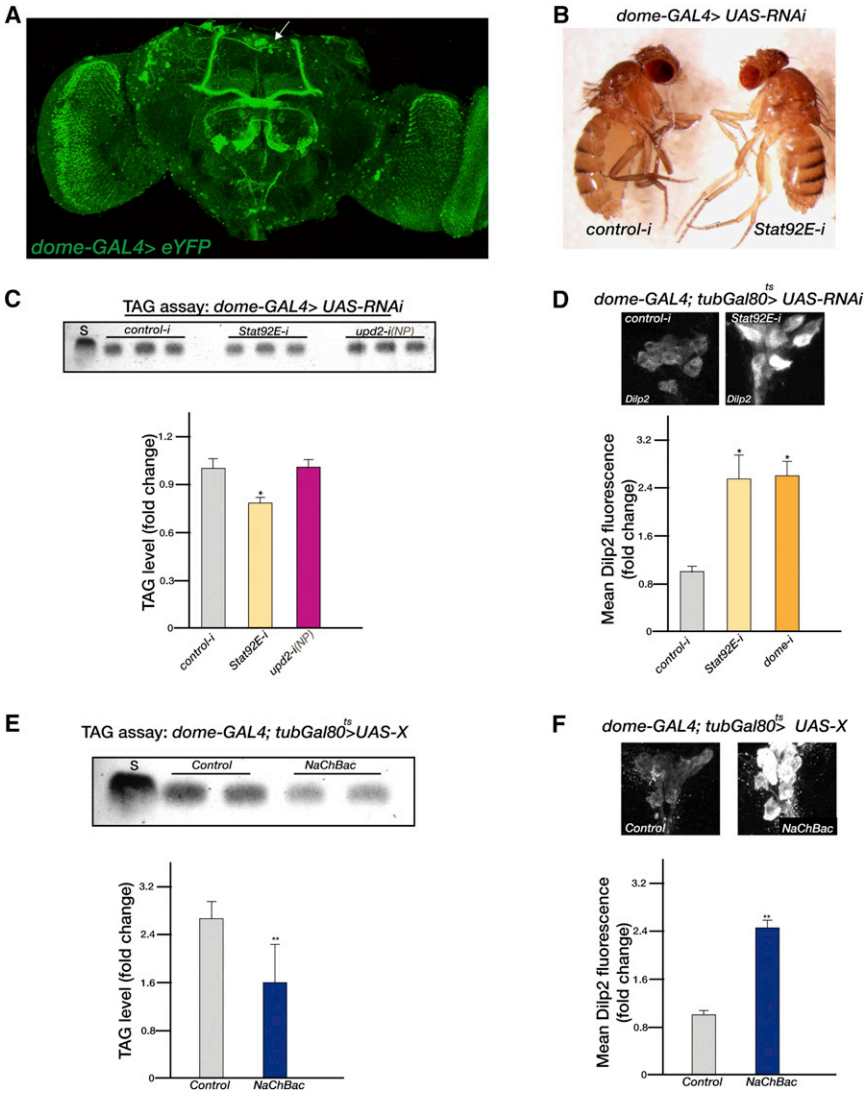

Figure 5. STAT Signaling in mNSC Neurons Regulates Systemic Growth and Metabolism

(A) MIP of adult female brain expressing enhanced *YFP* (*eYFP*) under the control of *dome-GAL4*. *dome-GAL4* is widely expressed and its expression domain includes a cluster of neurons in the mNSC region (white arrow).

(B) Expression of *STAT92E-RNAi* in the *dome-GAL4* expression domain results in small, slim flies.

(C) The amount of TAG measured by TLC is significantly reduced in adult females expressing *STAT92E-RNAi* with *dome-GAL4* but not with *upd2-RNAi*.

(D) Dilp2 fluorescence is significantly increased in both *STAT92E-RNAi* and *dome-RNAi* in the IPCs of adult females using *dome-Gal4*. The control in (B)–(D) is *GFP-RNAi*.

(E) The amount of TAG is significantly reduced in adult females expressing *NaChBac* with *dome-Gal4*.

(F) The expression of *NaChBac* in *dome-Gal4* neurons significantly increases Dilp2 accumulation in the IPCs of adult females. The control in (E) and (F) is *GFP* overexpression. Note that in (D)–(F), $Gal80^{ts}$ was used to allow transgene expression only in adults.

Error bars represent the SD; p values were calculated using Welch's t test (*$p < 0.05$, **$p << 0.01$, ***$p << 0.00001$).

Dilp release (Enell et al., 2010; Luo et al., 2012). Thus, we examined whether the cells in the mNSCs that express the STAT reporter could exert their effects through those neurotransmitter systems. However, although neurons that express the STAT reporter do not express the GABA receptor (Figure 6A), a subset of them expressed the *Drosophila* vesicular GABA transporter (dVGAT; Figure 6B, yellow arrows) that is required for GABA release (Fei et al., 2010). We found that reducing the activity of *dome* and *STAT* in dVGAT neurons affected systemic growth at 25°C (Figure 6C). Next, we assayed the level of stored fat in *dVGAT-GAL4 > dome-RNAi* adult flies at 29°C (because high levels of lethality were observed for *dVGAT-GAL4 > STAT-RNAi* at this temperature, we analyzed *dome* flies in the TAG and Dilp assays). The knockdown of *dome* in dVGAT neurons resulted in a significant decrease in stored fat (Figure 6D) and an increase in Dilp2 accumulation in the IPCs (Figure 6E), indicating that JAK/STAT signaling in GABAergic neurons relieves their inhibitory effect on IPCs. Consistent with our relay model, loss of JAK/STAT components in the Dilp neurons themselves did not affect systemic growth (data not shown) or metabolism (as assayed by stored fat; Figure S6).

Human Leptin Can Functionally Substitute for Upd2 by Signaling via the JAK/STAT Receptor Dome

Upd2 encodes a type I cytokine that presents structural features similar to those of Leptin (Boulay et al., 2003). Because our finding that Upd2 influences insulin secretion by impinging on STAT signaling in GABAergic neurons in order to disinhibit Dilp neurons is reminiscent of a recent finding that Leptin activates STAT signaling in GABAergic neurons and in turn results in the

(E and F) *upd2-RNAi* in the FB alters *STAT::GFP* reporter expression in the brain (F) compared with *Luciferase-RNAi* control (E). Note that the bouton-like enrichment of the *STAT::GFP* reporter along the neurites, juxtaposed with the IPCs, is lost in flies expressing FB-specific *upd2-RNAi* (compare yellow arrow in E with F). *STAT::GFP* expression in the cell body is reduced in flies expressing FB-specific *upd2-RNAi* (compare red arrow in E with F). Dilp2 fluorescence is increased in the IPCs of adult males expressing FB-specific *upd2-RNAi* compared with control (compare E with F).

See also Figures S3, S4, and S5.

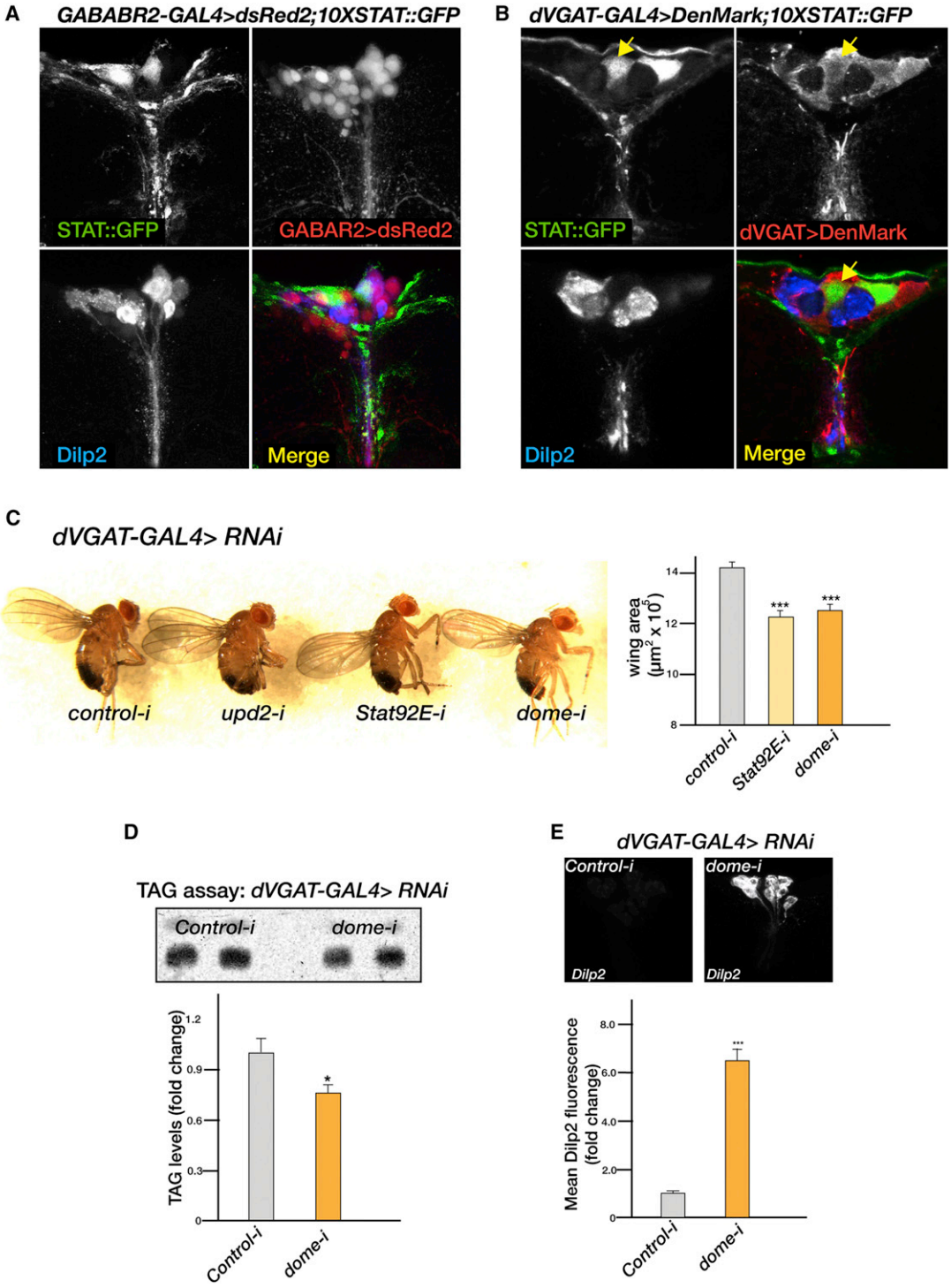

Figure 6. Role of the JAK/STAT Pathway in GABAergic Neurons Affects Systemic Growth and Metabolism by Influencing Dilp2 Accumulation in the IPCs

(A) XY slice of the mNSC region of *10XSTAT::GFP* male adult brains expressing *dsRed2* under the control of *GABA-B-R2-GAL4*. Immunostaining for Dilp2 (blue), GFP (green, *STAT::GFP* expression), and dsred2 (red, *GABA-B-R2* expression domain) shows that Dilp2 IPCs are positive for the GABA receptor, and that *STAT* reporter neurons do not overlap with the *GABA-B-R2-GAL4* expression domain.

(B) XY slice of the mNSC region of *10XSTAT::GFP* male adult brains expressing the membrane-associated dendritic marker DenMark under the control of the *dVGAT-GAL4* driver. Immunostaining for Dilp2 (blue), GFP (green, *STAT::GFP* expression), and DenMark (red, *dVGAT* expression domain) shows that *STAT* reporter neurons are positive for the vesicular GABA transporter dVGAT (yellow arrow).

derepression of a neuronal group called proopiomelanocortin (POMC) neurons, allowing them to fire (Vong et al., 2011), we tested the possibility that Leptin can substitute for Upd2. We generated transgenic flies that expressed human Leptin under the control of the UAS promoter (see Experimental Procedures) and expressed this transgene in the FB of *upd2Δ* flies. Strikingly, in similarity to flies expressing *upd2* cDNA in the FB, human *Leptin* cDNA was able to rescue the growth (Figure 7A), fat storage (Figure 7B), and Dilp2 accumulation phenotypes (Figure 7C) of *upd2Δ* flies. In addition, as documented in previous studies in mice (Caton et al., 2011; Ni et al., 2008; Rodgers and Shearn, 1977), injecting a physiologically relevant dose of recombinant human Leptin (see Experimental Procedures) into *upd2Δ* flies significantly reduced the accumulation of Dilp2 in *upd2Δ* brains (Figure 7D) and solved the primary defect underlying a loss of Upd2 function. These results suggest that exogenous Leptin signals through the same pathway as Upd2.

To test whether human Leptin is a bona fide ligand of the JAK/STAT pathway receptor Dome, we used a well-established JAK/STAT reporter assay (*10XSTATLuc*) in *Drosophila* Kc cells (Baeg et al., 2005; Hombría et al., 2005; Wright et al., 2011). *Drosophila* Kc cells were transfected with *10XSTATLuc* and Actin-promoter driving *Renilla luciferase* (*Act-Renilla*) together with dsRNAs against *dome* or control (*GFP*) or without dsRNA treatment. The cells were then incubated with 4 nM recombinant human Leptin, a concentration at which Upd ligands effectively activate the *10XSTATLuc* reporter in cell culture (Wright et al., 2011). We measured the ratio of firefly to *Renilla* luciferase activities (in relative luciferase units [RLUs]) at different time points after incubation with human Leptin, and compared it with the RLU of cells stimulated with media lacking Leptin. A significant increase in RLU in cells stimulated with Leptin over time was observed with control dsRNA or in cells not treated with dsRNAs (Figure 7E). However, cells treated with dsRNA against *dome* (two independent *dome* dsRNAs were used) were unable to respond to Leptin (Figure 7E). By plotting the luciferase signal as a function of the amount of human Leptin added, we found that the binding affinity (K_m-Michaelis constant) of human Leptin for Dome is 2.37 nM (Figure S7A), which is comparable to the K_m of 1 nM reported for the human Leptin receptor (DasGupta et al., 2005). These results provide strong evidence that human Leptin is able to signal through the JAK/STAT pathway in *Drosophila* cells by engaging the JAK/STAT receptor Dome.

DISCUSSION

Previous investigators have postulated the existence of secreted factors produced by the FB that stimulate systemic growth by stimulating cell proliferation, and proposed that the FB (the fly nutrient sensor) couples Dilp secretion from brain IPCs depending on the nutritional status (Britton and Edgar, 1998; Colombani et al., 2003; Davis and Shearn, 1977; Géminard et al., 2009). Here, we show that the JAK/STAT ligand Upd2, a type 1 cytokine signal, is involved in the interorgan communication between the FB and the brain IPCs. We demonstrate that human Leptin can rescue the *upd2* mutant phenotypes, which implies that an invertebrate model system can be used to address questions pertaining to Leptin biology.

Upd2 Plays an FB-Specific Role in Communicating the Fed State to the Brain IPCs

Upd proteins have secondary structures that are predicted to have α helices similar to that of type I cytokines belonging to the IL-6 family, and sequence alignments suggest that they show some similarity to vertebrate Leptins (Boulay et al., 2003; Harrison et al., 1998). Among the three Upd ligands that activate the Dome receptor, only Upd2 plays a significant role in communicating the nutritional status from the FB. This is somewhat surprising, because all three Upd proteins are secreted JAK/STAT pathway agonists and are able to activate the JAK/STAT pathway nonautonomously in vivo. However, the signal sequences of the different Upds appear to confer different biophysical properties upon them, as illustrated by tissue-culture assays showing that although Upd1 and Upd3 associate primarily with the extracellular matrix, Upd2 is easily detectable in the media (Wright et al., 2011). In addition, secretion assays showed that Upd2 is able to condition tissue-culture media more potently than either Upd1 or Upd3. Altogether, these results suggest that Upd2 activates JAK/STAT signaling at greater distances than Upd1 or Upd3.

As evidenced by the growth and metabolic phenotypes of FB-specific knockdown, Upd2 seems to be required only in the FB; however, the reason for this tissue specificity is unclear. In a previous study, Hombría et al. (2005) analyzed the Upd2 protein using a hidden Markov model, and suggested that Upd2 is probably not secreted via the classical Golgi-ER machinery because it lacks a signal peptide. In fact, other type I cytokines involved in interorgan crosstalk also lack the signal peptide and are secreted by unconventional secretory pathways (Haas et al., 2011). Thus, a possible explanation for the tissue specificity of Upd2 is that the FB is the only tissue that can secrete this protein in an active form. Future work, contingent on the development of techniques and reagents to detect Upd2 in the fly hemolymph, will clarify this issue.

Existence of Nutrient-Specific FB-Derived Signals

The identification of Upd2 as a nutrient-regulated signal from the FB that does not depend on AAs but is produced in response to dietary fats and sugars reveals that different nutrient-specific secreted factors exist in the fly. Of interest, the upregulation of *upd2* levels in FB knockdown of *slif* suggests the existence of a homeostatic feedback loop whereby Upd2, in the context of low protein, promotes the utilization of fat and carbohydrate energy sources. High-sugar diets in flies have been shown to

(C) Knockdown of *dome and STAT* in dVGAT neurons results in small, slim flies, as quantified by the reduction in wing area.
(D) The amount of TAG measured by TLC in adult males is significantly reduced when *dome-RNAi* is expressed with *dVGAT-GAL4*.
(E) Dilp2 fluorescence in IPCs is significantly increased when *dome* expression is compromised in the GABAergic neurons of adult males.
In (C)–(E) the control is *GFP-RNAi*. Error bars represent the SD; p values were calculated using Welch's t test (*$p < 0.05$, ***$p << 0.00001$). See also Figure S6.

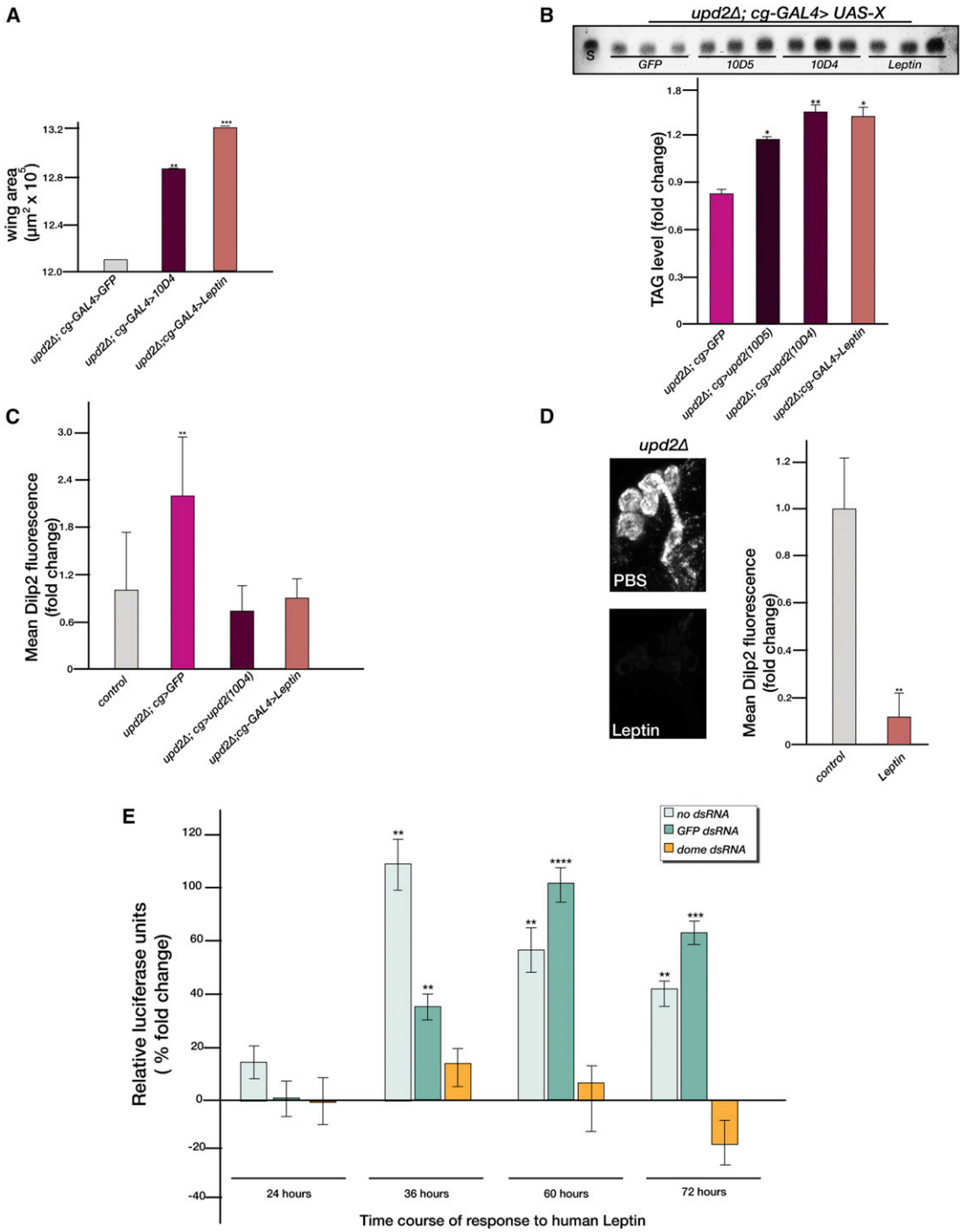

Figure 7. Human Leptin Can Rescue the *Upd2Δ* and Signals through Domeless

(A) Quantification of wing area in *upd2Δ* males with FB-specific expression of *upd2* cDNA (10D4) and human *Leptin* cDNA.

(B) The amount of TAG measured by TLC is significantly increased in adult males expressing human *Leptin* cDNA in the FB.

(C) Quantification of Dilp2 accumulation in FB-specific expression of the 10D4 *upd2* cDNA and human *Leptin* cDNA in *upd2Δ* background. Brains from *cg-Gal4* flies were used as positive controls (gray bar).

(D) MIP of *upd2Δ* adult male brains stained with Dilp2 after injection of human Leptin or control (PBS). The difference in Dilp2 fluorescence is quantified.

(E) Response of the *10XSTATLuc* reporter in Kc cells upon incubation with 4 nM human Leptin. The ratio of Renilla to firefly luciferase activity is measured at regular intervals from 24–72 hr and quantified as a percent fold change in relative units with respect to cells incubated with media alone in the presence of no dsRNA, control, or *dome* dsRNA.

Error bars represent the SD; p values were calculated using the t test (*p < 0.05, **p << 0.01, ***p < 0.001, ****p < 0.00001). See also Figure S7.

trigger a lipogenesis program akin to high-fat diets in mammals (Musselman et al., 2011; Zhou et al., 2005), suggesting that Upd2 is most likely downstream of signals that are produced by increased fat stores. This is a highly significant finding because it brings into question the broadly prevailing view that one dominant secreted factor downstream of AAs governs nearly all aspects of systemic growth and metabolism in flies. Our findings support a model in which the fly FB secretes numerous factors that regulate systemic growth and metabolism downstream of various components of the fly diet.

JAK/STAT Activation in GABAergic Neurons and Parallels the Adipose-Hypothalamic Circuit in Mammals

Our results indicate that STAT activation in GABAergic neurons inhibits their firing. Previous work implied that the GABA-B-receptors in Dilp neurons inhibit Dilp release (Enell et al., 2010). Given that these GABAergic neurons are presynaptic to the IPCs, we propose that activation of STAT in GABAergic neurons relieves the IPCs from repression, thus resulting in Dilp release. This is reminiscent of the observation that first-order neurons that respond to adipose-derived Leptin are inhibitory GABAergic neurons expressing LepRs (Vong et al., 2011). When LepRs are activated by Leptin, they regulate Stat3 phosphorylation, which inhibits the firing of the GABAergic neurons via an unknown mechanism. This in turn relieves the repression on the POMC neurons, allowing them to fire (Vong et al., 2011). Thus, this circuit module is strikingly similar to what we observe in the fly.

Many questions remain to be resolved regarding the signaling mechanisms by which the JAK/STAT pathway regulates GABAergic neurons. The target(s) of the JAK/STAT pathway in regulating neuronal firing in mammalian GABAergic neurons remains to be identified (Vong et al., 2011). It was suggested that Leptin activation of STAT signaling may be required for the long-term effects of Leptin's action on energy homeostasis, rather than for the acute effects of Leptin (Karsten et al., 2006), and that the acute effects of Leptin on the membrane potential of certain neuronal groups require activation of PI3-K signaling rather than STAT (Schober et al., 2005). However, the role of JAK/STAT versus PI3-K signaling in modulating the electrophysiology of the presynaptic GABAergic neurons has not yet been clarified (Vong et al., 2011), in large part because previous studies were done on non-GABAergic neuronal groups. Further investigations into the role of JAK/STAT signaling in modulating neurotransmission in GABAergic neurons will be necessary to clarify how JAK/STAT signaling regulates their activities. Of importance, based on the similarity of the circuits and the conservation of the signaling pathways, studies in the fly are likely to provide insights relevant to mammalian neurophysiology.

Parallels between Upd2 and Leptin

The physiology of Leptin signaling is undoubtedly more complex in vertebrates than in flies, and differs in several ways. For example, *upd2Δ* mutant flies are smaller and leaner, whereas mutations in Leptin in mammals are associated with obesity. However, there are some striking parallels. We find that under starvation, *upd2* mRNA steady-state levels drop significantly (Figure 2A), and there is a significant increase of *upd2* mRNA expression under high-fat diets (Figure 2F). This is similar to the alteration in Leptin levels observed during starvation and high-fat diets by Ahima et al. (1996). These authors examined the role of Leptin in the physiology of starvation by providing mice with exogenous Leptin during periods of nutrient restriction, and found that the primary physiological role of Leptin is to regulate the neuroendocrine system during starvation. Leptin reduced the animals' reproductive capacity and increased stress hormone levels, which in turn increased the survival capacity of the organism under adverse nutrient conditions (Ahima et al., 1996). Consistent with this, flies with ablated IPCs, which are unable to produce insulin, were shown to perform much better under starvation conditions and increased stress conditions (Broughton et al., 2005). Given that the role of Upd2 is to promote insulin secretion, the reduction of Upd2 levels during starvation should decrease Dilp secretion and increase the chances of survival under starvation (*upd2Δ* mutants were more starvation resistant than the wild-type controls; Figure S7B). Hence, in this context, the primary physiological roles of Upd2 and Leptin converge.

EXPERIMENTAL PROCEDURES

Drosophila Strains and Diets

Details about the fly strains, transgenic fly construction, standard lab food composition, and temperatures for specific crosses can be found in Extended Experimental Procedures.

Triglyceride Measurements

Triglyceride assays were performed as previously described (Al-Anzi et al., 2009). Further details can be found in Extended Experimental Procedures.

Hemolymph Glucose Measurements

Glucose concentration in the hemolymph was quantified as described previously (Géminard et al., 2009).

qPCR

Total RNA was prepared from triplicates of 15 fed (standard lab food) or starved (>72 hr on 1% sucrose agar) age-matched adult males at 25°C. cDNA was prepared using 1 μg RNA, and qPCR was performed using iQ SYBR Green Supermix. *alpha-tubulin* and *rp49* were used to normalize the RNA levels. Relative quantification of mRNA levels was calculated using the comparative C_T method. See Extended Experimental Procedures for information on the oligos.

Feeding Assays

The blue dye feeding assay was adapted from Xu et al. (2008). The CAFÉ assay was performed as described by Ja et al. (2007).

Oil Red O Staining

Oil Red O staining was performed as previously described (Gutierrez et al., 2007; Palanker et al., 2009).

Immunostaining, Confocal Imaging, and Analysis

Immunostaining of larval and adult brains was performed based on protocols described by Pfeiffer et al. (2010). Images were captured with the use of Leica SP2 and Zeiss LSM 780 confocal systems, and analyzed using Zeiss ZenLite 2009, Leica LAS AF lite, and ImageJ. To calculate the intensity of Dilp staining, the mean gray value was calculated from maximum intensity projections (MIPs) of a similar number of confocal stacks using ImageJ. For details on the antibodies used, see Extended Experimental Procedures.

Leptin Injections

Human recombinant Leptin (#L4146-1MG; Sigma Aldrich) was dissolved per the package instructions in a solution of Hcl and NaOH to a final concentration of 1 μg/μl to prepare the human Leptin stock solution, which was then frozen in aliquots at −20°C. Fresh aliquots were thawed on ice before each experiment. The working solution was made by diluting the human Leptin stock solution in PBS to a final concentration of 0.001 μg/μl and injected into 10-day-old adult males of *y w* and *upd2Δ*. PBS was injected into mock controls. The injections were done by inserting the needle at the junction of the thorax and abdomen close to the haltere using a microinjector (Femtoget; Eppendorf) at a pressure of 305 kPa, using needles pulled in a pipette puller (vertical pipette puller, model 720; Kopf) at a heater setting of 14.1. At least 25–20 flies were injected per condition. The flies were allowed to recover for 24 hr and then the brains were dissected, stained, and analyzed, and Dilp2 levels were quantified as outlined in the previous section. A minimum of three to five brains were analyzed per experiment. The experiments were performed three independent times.

Tissue-Culture and Luciferase Assays

Drosophila Kc cells were maintained in Schneider's medium (GIBCO), 10% heat-inactivated fetal bovine serum (FBS; Sigma), and 5% Pen-Strep (GIBCO) at 25°C. Experiments were run in 96-well plates (in six replicates per condition), and 150 ng/uL of the appropriate dsRNA were seeded in the wells before the start of the experiment. Each well was transfected with 0.05 ng *10XSTATLuc*, 14 ng *Act-Renilla*, and 106 ng pAC-PL (used as carrier DNA). Then, 96 hr after transfection, media supplemented with 4 nM human recombinant Leptin or control media supplemented with no Leptin were added to the wells. Luciferase activity was measured using DualGlo reagents (Promega) per the kit instructions and measured using the Analyst GT plate reader. For details about the amplicons used for dsRNA production, refer to Extended Experimental Procedures.

Statistical Analysis

Statistical analysis was performed using Welch's t test with Excel.

SUPPLEMENTAL INFORMATION

Supplemental Information includes Extended Experimental Procedures and seven figures and can be found with this article online at http://dx.doi.org/10.1016/j.cell.2012.08.019.

ACKNOWLEDGMENTS

We thank M. Zeidler, E. Bach, B. Hassan, B. White, B. Al-Anzi, M. Pankratz, P. Shen, J. Wang, D. Krantz, J. Simpson, A. Gould, E. Hafen, H. Stocker, P. Leopold, G. Technau, and E. Olson for reagents. We thank the Transgenic RNAi Resource Project, NIG-Fly Stock Center (Japan), and the Bloomington Stock Center for flies, the Developmental Studies Hybridoma Bank for monoclonal antibodies, and the *Drosophila* RNAi Screening Center (Harvard Medical School) for dsRNA reagents and plate-reader equipment. We also thank C. Villalta for performing embryonic microinjections to create the human Leptin transgenic flies, F. Demontis and C. Pitsouli for critical comments on the manuscript, Y. Kwon for advice on the STAT luciferase assay, I. Droujinine for discussions and help with the diet experiments, and P. Raghavan and F. Wirtz-Peitz for insightful comments and discussions during the course of this work. This work was supported by the National Institutes of Health (5P01CA120964 and 5R01DK088718). N.P. is a Howard Hughes Medical Institute investigator.

Received: March 13, 2012
Revised: June 1, 2012
Accepted: August 6, 2012
Published: September 27, 2012

REFERENCES

Ahima, R.S., Prabakaran, D., Mantzoros, C., Qu, D., Lowell, B., Maratos-Flier, E., and Flier, J.S. (1996). Role of leptin in the neuroendocrine response to fasting. Nature *382*, 250–252.

Al-Anzi, B., Sapin, V., Waters, C., Zinn, K., Wyman, R.J., and Benzer, S. (2009). Obesity-blocking neurons in *Drosophila*. Neuron *63*, 329–341.

Bach, E.A., Ekas, L.A., Ayala-Camargo, A., Flaherty, M.S., Lee, H., Perrimon, N., and Baeg, G.H. (2007). GFP reporters detect the activation of the *Drosophila* JAK/STAT pathway in vivo. Gene Expr. Patterns *7*, 323–331.

Baeg, G.H., Zhou, R., and Perrimon, N. (2005). Genome-wide RNAi analysis of JAK/STAT signaling components in *Drosophila*. Genes Dev. *19*, 1861–1870.

Binari, R., and Perrimon, N. (1994). Stripe-specific regulation of pair-rule genes by hopscotch, a putative Jak family tyrosine kinase in *Drosophila*. Genes Dev. *8*, 300–312.

Boulay, J.L., O'Shea, J.J., and Paul, W.E. (2003). Molecular phylogeny within type I cytokines and their cognate receptors. Immunity *19*, 159–163.

Britton, J.S., and Edgar, B.A. (1998). Environmental control of the cell cycle in *Drosophila*: nutrition activates mitotic and endoreplicative cells by distinct mechanisms. Development *125*, 2149–2158.

Brogiolo, W., Stocker, H., Ikeya, T., Rintelen, F., Fernandez, R., and Hafen, E. (2001). An evolutionarily conserved function of the *Drosophila* insulin receptor and insulin-like peptides in growth control. Curr. Biol. *11*, 213–221.

Broughton, S.J., Piper, M.D., Ikeya, T., Bass, T.M., Jacobson, J., Driege, Y., Martinez, P., Hafen, E., Withers, D.J., Leevers, S.J., and Partridge, L. (2005). Longer lifespan, altered metabolism, and stress resistance in *Drosophila* from ablation of cells making insulin-like ligands. Proc. Natl. Acad. Sci. USA *102*, 3105–3110.

Brown, S., Hu, N., and Hombría, J.C. (2001). Identification of the first invertebrate interleukin JAK/STAT receptor, the *Drosophila* gene domeless. Curr. Biol. *11*, 1700–1705.

Caton, P.W., Kieswich, J., Yaqoob, M.M., Holness, M.J., and Sugden, M.C. (2011). Nicotinamide mononucleotide protects against pro-inflammatory cytokine-mediated impairment of mouse islet function. Diabetologia *54*, 3083–3092.

Colombani, J., Raisin, S., Pantalacci, S., Radimerski, T., Montagne, J., and Léopold, P. (2003). A nutrient sensor mechanism controls *Drosophila* growth. Cell *114*, 739–749.

DasGupta, R., Boutros, M., and Perrimon, N. (2005). *Drosophila* Wnt/Fz pathways. Sci. STKE *2005*, cm5.

Davis, K.T., and Shearn, A. (1977). In vitro growth of imaginal disks from *Drosophila melanogaster*. Science *196*, 438–440.

Dinarello, C.A., and Mier, J.W. (1986). Interleukins. Annu. Rev. Med. *37*, 173–178.

Enell, L.E., Kapan, N., Söderberg, J.A., Kahsai, L., and Nässel, D.R. (2010). Insulin signaling, lifespan and stress resistance are modulated by metabotropic GABA receptors on insulin producing cells in the brain of *Drosophila*. PLoS ONE *5*, e15780.

Fei, H., Chow, D.M., Chen, A., Romero-Calderón, R., Ong, W.S., Ackerson, L.C., Maidment, N.T., Simpson, J.H., Frye, M.A., and Krantz, D.E. (2010). Mutation of the *Drosophila* vesicular GABA transporter disrupts visual figure detection. J. Exp. Biol. *213*, 1717–1730.

Géminard, C., Rulifson, E.J., and Léopold, P. (2009). Remote control of insulin secretion by fat cells in *Drosophila*. Cell Metab. *10*, 199–207.

Gutierrez, E., Wiggins, D., Fielding, B., and Gould, A.P. (2007). Specialized hepatocyte-like cells regulate *Drosophila* lipid metabolism. Nature *445*, 275–280.

Haas, Y., Windig, J.J., Calus, M.P., Dijkstra, J., Haan, M., Bannink, A., and Veerkamp, R.F. (2011). Genetic parameters for predicted methane production and potential for reducing enteric emissions through genomic selection. J. Dairy Sci. *94*, 6122–6134.

Harrison, D.A., McCoon, P.E., Binari, R., Gilman, M., and Perrimon, N. (1998). *Drosophila* unpaired encodes a secreted protein that activates the JAK signaling pathway. Genes Dev. *12*, 3252–3263.

Hombría, J.C., Brown, S., Häder, S., and Zeidler, M.P. (2005). Characterisation of Upd2, a *Drosophila* JAK/STAT pathway ligand. Dev. Biol. *288*, 420–433.

Hou, X.S., Melnick, M.B., and Perrimon, N. (1996). Marelle acts downstream of the *Drosophila* HOP/JAK kinase and encodes a protein similar to the mammalian STATs. Cell *84*, 411–419.

Hursting, S.D., Lavigne, J.A., Berrigan, D., Perkins, S.N., and Barrett, J.C. (2003). Calorie restriction, aging, and cancer prevention: mechanisms of action and applicability to humans. Annu. Rev. Med. *54*, 131–152.

Ikeya, T., Galic, M., Belawat, P., Nairz, K., and Hafen, E. (2002). Nutrient-dependent expression of insulin-like peptides from neuroendocrine cells in the CNS contributes to growth regulation in *Drosophila*. Curr. Biol. *12*, 1293–1300.

Ja, W.W., Carvalho, G.B., Mak, E.M., de la Rosa, N.N., Fang, A.Y., Liong, J.C., Brummel, T., and Benzer, S. (2007). Prandiology of *Drosophila* and the CAFE assay. Proc. Natl. Acad. Sci. USA *104*, 8253–8256.

Kahn, C.R., King, G.L., Moses, A.C., Weir, G.C., Jacobson, A.M., and Smith, R.J. (2005). Joslin's Diabetes Mellitus, 14th edition (Boston: Lippincott Williams & Wilkins).

Karsten, P., Plischke, I., Perrimon, N., and Zeidler, M.P. (2006). Mutational analysis reveals separable DNA binding and trans-activation of *Drosophila* STAT92E. Cell. Signal. *18*, 819–829.

Klagges, B.R., Heimbeck, G., Godenschwege, T.A., Hofbauer, A., Pflugfelder, G.O., Reifegerste, R., Reisch, D., Schaupp, M., Buchner, S., and Buchner, E. (1996). Invertebrate synapsins: a single gene codes for several isoforms in *Drosophila*. J. Neurosci. *16*, 3154–3165.

Kulkarni, R.N., Wang, Z.L., Wang, R.M., Hurley, J.D., Smith, D.M., Ghatei, M.A., Withers, D.J., Gardiner, J.V., Bailey, C.J., and Bloom, S.R. (1997). Leptin rapidly suppresses insulin release from insulinoma cells, rat and human islets and, in vivo, in mice. J. Clin. Invest. *100*, 2729–2736.

Luan, H., Lemon, W.C., Peabody, N.C., Pohl, J.B., Zelensky, P.K., Wang, D., Nitabach, M.N., Holmes, T.C., and White, B.H. (2006). Functional dissection of a neuronal network required for cuticle tanning and wing expansion in *Drosophila*. J. Neurosci. *26*, 573–584.

Luo, J., Becnel, J., Nichols, C.D., and Nässel, D.R. (2012). Insulin-producing cells in the brain of adult *Drosophila* are regulated by the serotonin 5-HT1A receptor. Cell. Mol. Life Sci. *69*, 471–484.

Mandal, L., Martinez-Agosto, J.A., Evans, C.J., Hartenstein, V., and Banerjee, U. (2007). A Hedgehog- and Antennapedia-dependent niche maintains *Drosophila* haematopoietic precursors. Nature *446*, 320–324.

Morton, G.J., Cummings, D.E., Baskin, D.G., Barsh, G.S., and Schwartz, M.W. (2006). Central nervous system control of food intake and body weight. Nature *443*, 289–295.

Musselman, L.P., Fink, J.L., Narzinski, K., Ramachandran, P.V., Hathiramani, S.S., Cagan, R.L., and Baranski, T.J. (2011). A high-sugar diet produces obesity and insulin resistance in wild-type *Drosophila*. Disease Models Mech. *4*, 842–849.

Ni, J.Q., Markstein, M., Binari, R., Pfeiffer, B., Liu, L.P., Villalta, C., Booker, M., Perkins, L., and Perrimon, N. (2008). Vector and parameters for targeted transgenic RNA interference in *Drosophila melanogaster*. Nat. Methods *5*, 49–51.

Palanker, L., Tennessen, J.M., Lam, G., and Thummel, C.S. (2009). *Drosophila* HNF4 regulates lipid mobilization and beta-oxidation. Cell Metab. *9*, 228–239.

Pfeiffer, B.D., Ngo, T.T., Hibbard, K.L., Murphy, C., Jenett, A., Truman, J.W., and Rubin, G.M. (2010). Refinement of tools for targeted gene expression in *Drosophila*. Genetics *186*, 735–755.

Ren, D., Navarro, B., Xu, H., Yue, L., Shi, Q., and Clapham, D.E. (2001). A prokaryotic voltage-gated sodium channel. Science *294*, 2372–2375.

Rodgers, M.E., and Shearn, A. (1977). Patterns of protein synthesis in imaginal discs of *Drosophila melanogaster*. Cell *12*, 915–921.

Rulifson, E.J., Kim, S.K., and Nusse, R. (2002). Ablation of insulin-producing neurons in flies: growth and diabetic phenotypes. Science *296*, 1118–1120.

Schober, M., Rebay, I., and Perrimon, N. (2005). Function of the ETS transcription factor Yan in border cell migration. Development *132*, 3493–3504.

Taguchi, A., and White, M.F. (2008). Insulin-like signaling, nutrient homeostasis, and life span. Annu. Rev. Physiol. *70*, 191–212.

Vong, L., Ye, C., Yang, Z., Choi, B., Chua, S., Jr., and Lowell, B.B. (2011). Leptin action on GABAergic neurons prevents obesity and reduces inhibitory tone to POMC neurons. Neuron *71*, 142–154.

White, B.H., Osterwalder, T.P., Yoon, K.S., Joiner, W.J., Whim, M.D., Kaczmarek, L.K., and Keshishian, H. (2001). Targeted attenuation of electrical activity in *Drosophila* using a genetically modified K(+) channel. Neuron *31*, 699–711.

Wright, V.M., Vogt, K.L., Smythe, E., and Zeidler, M.P. (2011). Differential activities of the *Drosophila* JAK/STAT pathway ligands Upd, Upd2 and Upd3. Cell. Signal. *23*, 920–927.

Wu, Q., and Brown, M.R. (2006). Signaling and function of insulin-like peptides in insects. Annu. Rev. Entomol. *51*, 1–24.

Xu, K., Zheng, X., and Sehgal, A. (2008). Regulation of feeding and metabolism by neuronal and peripheral clocks in *Drosophila*. Cell Metab. *8*, 289–300.

Zeidler, M.P., Bach, E.A., and Perrimon, N. (2000). The roles of the *Drosophila* JAK/STAT pathway. Oncogene *19*, 2598–2606.

Zhang, Y., Proenca, R., Maffei, M., Barone, M., Leopold, L., and Friedman, J.M. (1994). Positional cloning of the mouse obese gene and its human homologue. Nature *372*, 425–432.

Zhou, X., Liu, K.Y., Bradley, P., Perrimon, N., and Wong, S.T. (2005). Towards automated cellular image segmentation for RNAi genome-wide screening. Med. Image Comput. Comput. Assist. Inter. *8*, 885–892.

Cell

EXTENDED EXPERIMENTAL PROCEDURES

Drosophila Strains

The *upd2* homozygous deletion mutant used is *upd2*$^{\Delta 3\text{-}62}$ (*upd2Δ*; Hombría et al., 2005). STAT reporter flies- 10XSTAT::GFP (Bach et al., 2007). UAS lines are: *UAS-upd2-GFP* (transgenic lines 10D4 and 10D5; Hombría et al., 2005); *UAS-slif*^{anti} (Colombani et al., 2003); *UAS-Src::GFP* (Bloomington Stock #*5432)*; *UAS-dsRed2* (Bloomington Stock #8546*); UAS-DenMark* (Nicolaï et al., 2010); *UAS-NaChBac* (Luan et al., 2006); and *UAS-EKO222* (White et al., 2001). Gal4 lines are: *cg-GAL4* (Hennig et al., 2006); *ppl-GAL4* (Zinke et al., 1999); *yolk-GAL4* (Georgel et al., 2001); *Dilp2-GAL4* (Wu et al., 2005); *Dilp3-GAL4* (Buch et al., 2008); *dome-Gal4*, *UAS-2xEYFP* (Mandal et al., 2007); *GABA-B-R2-GAL4* (Enell et al., 2010); *dVGAT-GAL4* (Fei et al., 2010); and *Dmef2-GAL4* (Ranganayakulu et al., 1996). RNAi lines from the TRiP facility at Harvard Medical School (http://www.flyrnai.org/TRiP-HOME.html) are: *Luciferase-RNAi* (JF01801); *white-RNAi* (JF01786); *GFP-RNAi* (HMS00314); *upd1-RNAi* (JF03149); *upd3-RNAi* (HMS05061); upd2-RNAi (HMS00901) [referred to as upd2-RNAi (NP)]; *STAT92E-RNAi* (HMS00035); and *dome-RNAi* (HMS00647). RNAi lines from the National Institute of Genetics, Japan are: *upd2-RNAi* (5988R-1) [referred to as *upd2(1)-RNAi*] and *upd2-RNAi* (5988R-3) [referred to as *upd2(2)-RNAi*].

Food and Temperature

Flies were raised on standard lab food containing 15 g yeast, 8.6 g soy flour, 63 g corn flour, 5g agar, 5g malt, 74 ml corn syrup per liter. Temperature regiments for specific crosses were: 18C: *dome-GAL4 > STAT-RNAi* and *upd2-RNAi, dome-GAL4; tubGAL80*^{ts} > *UAS-RNAi* and *UAS-GFP/NaChBac*. Once adults eclosed, they were shifted to 29C for 3-7 days before performing the assays. 25C: *y w* and *upd2Δ*, *cg-GAL4 > UAS-RNAi* and *UAS-overexpression*, *upd2Δ; cg-GAL4 > UAS-overexpression* rescue crosses, *upd2Δ; Dilp3-GAL4 > UAS-NaChBac/EKO222/GFP*, *ppl-GAL4 > UAS-RNAi; 10XSTAT::GFP.* 27C: *ppl-GAL4 > UAS-RNAi.* 29C: *yolk-GAL4 > UAS-RNAi.* For acute 24 hr starvation experiments (Figures 2G and 2H), 3-7 day old male flies were kept on 1% agar at 29C. For chronic starvation experiments (Figures 2A, 4C, and 4D), 3-7 day old male flies were kept on 1% sucrose agar at 25C.

Analysis of Cell Size and Number

Control and experimental flies were obtained from vials of similar population density. Wings clipped from adult male flies were imaged using differential interference contrast microscopy (Zeiss Axioskop2). Wing area was measured using ImageJ and cell number measured using Adobe photoshop CS5 by counting the number of wing hairs in 40 × 40 μm squares. Cell density was measured by dividing the number of cells by wing area.

Triglyceride Measurements

Colorimetric assay

Three to five replicates of 20 male larvae or decapitated adult flies (10 females or 15 males) of a given genotype were homogenized in 250 μl of 0.1% Triton X-100 in the presence of a protease inhibitor (EDTA-free Complete, Roche, #11836170001). Samples were centrifuged at 14,000 rpm in a refrigerated tabletop centrifuge. 10.0 μl of the supernatant was used to determine the level of TAG in the sample using the Stanbio LiquiColor triglyceride Test kit (Stanbio, #2100-225) and 100.0 μl of the supernatant was used to measure the amount of protein in the sample using the BCA assay kit (Pierce, #23221).

TLC assay

Two to three replicates of five adult males or females of a given genotype were homogenized in 100 μl of 2:1 chloroform methanol mixture. The samples were briefly centrifuged at 8,000 rpm in a refrigerated centrifuge. Coconut oil (20uL dissolved in 1 ml of 2:1 chloroform-methanol mixture) was used as standard. 2 μl of the sample and standard were loaded onto a silica gel TLC plate (Sigma Aldrich, # 70644) and run in a chamber using 4:1 hexane and ethyl ether as the mobile phase. The plate was then dipped in a general oxidizing stain for 30 s. The oxidizing ceric ammonium molybdate stain was made by dissolving 8.75 g ammonium heptamolybdate tetrahydrate (Sigma Aldrich, 431346-50G) and 3.5g Cerium(IV) sulfate hydrate (Sigma Aldrich, # 423351) in 35 ml of concentrated sulphuric acid and 315 ml of water. The plate was developed in an oven at 85–90°C for 15 min. Each experiment was run on at least three independent silica plates. The plates were scanned and analyzed using Adobe photoshop CS5. To quantify TAG levels and control for loading, the ratio of the ''gray value'' function of the TAG band to another band along the same lane was used as a measure. An average of the ratio obtained from at least three technical replicates per lane was used as a measure of the TAG level per replicate.

Hemolymph Glucose Measurements

Quantification of glucose concentration in the hemolymph was done as described in (Géminard et al., 2009). Triplicates of 10 adult females of the indicated genotypes were decapitated, placed in a perforated 0.5 ml tube, centrifuged for 6 min at 1,500 g, and the hemolymph collected in an underlying 1.5 ml tube at 4C. The hemolymph was diluted 1:10 in distilled water and the glucose concentration was determined using the Glucose Hexokinase Assay kit (Sigma #GAHK-20) after trehalose conversion into glucose with porcine trehalase (Sigma #T8778) and incubation at 37C overnight.

qPCR

Total RNA was prepared from triplicates of 15 fed (standard lab food) or starved (>72 hr on 1% sucrose agar), age-matched adult males at 25C. RNA was extracted using Trizol, treated with DNAase-I (QIAGEN #79254), and cleaned up using the RNeasy MinElute Cleanup Kit (QIAGEN # 74204). cDNA was prepared using iScript cDNA Synthesis (Bio-Rad, #1708891) and 1 μg RNA was used per reaction. qPCR was performed using iQ SYBR Green Supermix (Bio-Rad, # 1708882). *alpha-tubulin* and *rp49* were used to normalize the RNA levels. Relative quantification of mRNA levels was calculated using the comparative C_T method. List of primers:

rp49: 5′- ATCGGTTACGGATCGAACAA −3′ and 5′- GACAATCTCCTTGCGCTTCT-3′. *alpha-tubulin*: 5′-GCTGTTCCACCCCGA GCAGCTGATC-3′ and 5′-GGCGAACTCCAGCTTGGACTTCTTGC-3′.
STAT92E: 5′-CTGGGCATTCACAACAATCCAC-3′ and 5′-GTATTGCGCGTAACGAACCG-3′.
upd2: 5′- CGGAACATCACGATGAGCGAAT-3′ and 5′- TCGGCAGGAACTTGTACTCG-3′.

For Figure S2, total RNA was extracted in triplicates, each consisting of 15 larval brains dissected from male larvae which had either a knockdown of *upd2* or control (*GFP-RNAi*). The qPCR was performed as described in the main Experimental Procedures. The primers used for Dilp2 mRNA are: 5′- GAATCACGGGATTATACTCCTCG −3′ and 5′- ATGAGCAAGCCTTTGTCCTTCA −3′.

Feeding Assays

Blue dye assay

Feeding assay was adapted from (Xu et al., 2008). Briefly, three to five replicates 5 adult males or females (3-7 days old) of the indicated genotype were provided food with blue dye (15% sucrose, 1% agar and 1% brilliant blue) for 4 hr at 25°C. The flies were then decapitated and the torso was homogenized in 500 μl of PBS, the samples were then centrifuged at 13,000 rpm in a tabletop centrifuge for 20 mins. The supernatant was then used to measure absorbance at a wavelength of 625 nm.

CAFÉ assay

The CAFÉ assay was performed as described in (Ja et al., 2007). 16 hr before the assay, five replicates per genotype of 7 adult male flies (3–7 days old) were transferred from standard lab food to 1.0% agar vials and provided with a 2.5% yeast extract and 5% sucrose solution maintained in 5 ml calibrated glass micropipettes (VWR, #53432-706). At the start of the assay, the old micropipette was replaced with a new one. The amount of liquid food consumed was recorded every 2 hr and corrected on the basis of the evaporation observed in a vial without flies.

Oil Red O Staining

To prepare the 0.5% oil red O stain, 0.125 g of Oil red O (Sigma Aldrich, #0625-25G) was dissolved in 25 ml of 100% propylene glycol, heated gently in a water bath until temperature of the solution reached 95°C. It was then filtered through whatman paper (25 μM pore size) while still warm and allowed to cool to room temperature (RT) overnight. The oil red O staining was performed as previously described (Gutierrez et al., 2007; Palanker et al., 2009). Actively feeding larvae from *y w* and *upd2Δ* on standard lab food were dissected and samples fixed in 4% formaldehyde in PBS for 30 min. The tissue was then washed twice in PBS, twice in 100% propylene glycol and incubated at 65C for 10 min in 0.5% oil red O stain prewarmed to 65C. The tissue was then cleared by rinsing in 85% propylene glycol and mounted in 75% glycerol. Differential interference contrast images were then obtained using a Zeiss Axioskop2 microscope.

Immunostaining, Confocal Imaging, and Analysis

Immunostaining of larval and adult brains were performed based on protocols from (Pfeiffer et al., 2010). Primary antibodies used are: rat-anti-Dilp2 (1:200; Géminard et al., 2009), rabbit-anti-Dilp5 (1:800; Géminard et al., 2009), chicken-anti-GFP (1:2,000, Abcam, # ab13970), and mouse anti-nc82 (1:10, DSHB, # nc82 s1). Secondary antibodies used are: donkey anti-rat DyLight 649 (Jackson ImmunoResearch Labs, # 712-495-150; donkey anti-chicken Dylight 488 (Jackson ImmunoResearch Labs, # 703-485-155); and donkey anti-mouse Alexa 594 (Invitrogen, # A-21203). Additional primary antibodies used in the supplemental experiments are: Rat-Elav (1:500; O'Neill et al., 1994; DSHB #7E8A10); Rabbit- Repo (1:1,000; Halter et al., 1995; gift of G.M. Technau, University of Mainz, Germany); Mouse-Synapsin (1:10; Klagges et al., 1996; DSHB #3C11). Confocal images were analyzed using Zeiss ZenLite 2009, Leica LAS AF lite and ImageJ. To calculate the intensity of Dilp staining, mean gray value was calculated from MIPs of a similar number of confocal stacks using ImageJ.

Larval Stainings

Larval brains were dissected and fixed for 30 min in 4% formaldehyde in PBS, washed multiple times in PBS with 1% Triton X-100 (PBT) + 0.5% BSA. Tissues were then preblocked in PBT + 0.5% BSA + 5% Normal donkey serum (NDS) (referred to as block) for 1 hr and then incubated overnight at 4C with the primary antibody in block, and then washed multiple times in PBT+0.5% BSA and incubated for 30 min in block. A cocktail of secondary antibodies was then added to the block (final concentration 1:250) and the tissues were incubated in secondary for 2-4 hr at RT. The samples were then washed 3× for 15 min each time, with PBT+0.5% BSA and mounted on slides with a single scotch tape spacer in Slowfade gold antifade (Invitrogen, # S36936). Brains were imaged using Leica SP2 confocal system. Regarding the Dilp staining in larvae, when larvae are in the postfeeding state, just prior to pupariation, they already have an increase in basal levels of Dilp accumulation (Slaidina et al., 2009); hence, the sensitivity of this assay is

compromised. The difference is most prominent in actively feeding larvae. Matching the sex and population density is also crucial to detect a significant difference in Dilp accumulation.

Adult Stainings

Adult brains were dissected in PBS and fixed in cold 0.8% Para-formaldehyde (PFA) in PBS overnight at 4C. Tissues were washed the following day multiple times in 0.5% BSA and 0.5% Triton X-100 in PBS (PAT), preblocked in PAT+ 5% NDS for 2 hr at RT, and then incubated with the primary antibody overnight at 4C. The following day, the tissues were washed numerous times in PAT and then blocked again for 30 min in PAT+ 5% NDS and incubated in a cocktail of secondary antibodies in block (final concentration of 1:500) overnight at 4C. The samples were washed 3×–5× for 15 min per wash in PAT and mounted on slides with two layers of scotch tape spacers in Slowfade gold antifade (Invitrogen, #S36936) and imaged using Leica SP2 and Zeiss LSM 780 confocal systems.

Construction of Human Leptin Transgenic Flies

Leptin human cDNA clone was obtained (Origene, # SC120021, LEP [NM_000230]) and the Leptin ORF was PCR amplified using a high fidelity PCR polymerase (Bio-Rad, #172-5330). Primers used were 5′– caacatgggaATGCATTGGGGAACCCTGTG –3′ and 5′ –TCAGCATCCAGGGCTGAGGTCCAGCTG –3′. The PCR product was then cloned into the pWALIUM10-roe vector available from the TRiP facility at Harvard Medical School. The cloning was performed as per the protocol listed on the TRiP website (http://www.flyrnai.org/supplement/VALIUM10roe_Protocol.pdf). Briefly, the PCR product cloned into the gateway vector pENTR/D TOPO vector (Invitrogen, K240020). The entry plasmid pENTR-Leptin was then used in a LR clonase reaction (Invitrogen, 11791-020), with the destination vector pWALIUM10-roe (Ni et al., 2008). The plasmid was then microinjected into embryos which harbor attP2 landing sites, as per standard procedures to create transgenics. Two independent germline transformed lines were established from 50 injected embryos in the *y w* background.

Tissue-Culture and Luciferase Assays

Drosophila Kc cells were maintained in Schneider's medium (GIBCO), 10% heat-inactivated FBS (SIGMA) and 5% Pen-Strep (GIBCO) at 25°C. The day before transfection cells were passaged to 60%–80% confluency. Experiments were run in 96 well plates (in six replicates per condition), 150 ng/μl of the appropriate dsRNA (GFP (control) or *dome* (DRSC amplicon IDs– DR19583 and DR32731) prepared using the MegaScript in vitro transcription kit (Ambion) were seeded in the wells prior to the start of experiment. Each well was transfected with 0.05 ng *10XSTATLuc*, 14 ng *Act-Renilla*, 106 ng pAC-PL (used as carrier DNA), the above DNA master mix was mixed with 21.5 μl of EC buffer (QIAGEN), incubated for 2-3 min at RT, then mixed with 2.5 μl Enhancer (QIAGEN), incubated for 2–3 min at RT, then mixed with 0.75 μl Effectene transfection reagent (QIAGEN) and dispensed into the wells. The dsRNA and DNA transfection mix was incubated in the wells at RT for 5–10 min and then 100 μl Kc cells were added per well at a concentration of 3×10^4 cells. 96 hr after transfection, media supplemented with 4 nM human recombinant Leptin (Sigma Aldrich, # L4146-1MG) or control media supplemented with no Leptin was added to the wells. Luciferase activity was measured using DualGlo reagents (Promega) as per kit instructions and measured using the Analyst GT plate reader.

Calculation of the Michaelis Constant K_m of Leptin

The experimental procedure followed for the cell-based luciferase was the same as described above. The experiment was done in six replicates with four different doses of human Leptin and luciferase activity was measured 30 hr after stimulation with Leptin. The response of 10XSTATLuc reporter at different doses of human Leptin in Kc Cells was determined. The fold change in the RLU of the STAT reporter at different doses of human Leptin was plotted. A logarithmic trend-line fitted the data with a correlation coefficient of 0.93. K_m is the substrate concentration at which the reaction rate is half of V_{max}, the maximum rate achieved by the system. In this experimental data set the V_{max} was 32.8 at 40 nM of human Leptin. Solving the equation of this log curve, $y = 21.188 \ln(x) - 1.8226$, yielded a K_m for human Leptin in this assay to be 2.37 nM.

SUPPLEMENTAL REFERENCES

Bach, E.A., Ekas, L.A., Ayala-Camargo, A., Flaherty, M.S., Lee, H., Perrimon, N., and Baeg, G.H. (2007). GFP reporters detect the activation of the *Drosophila* JAK/STAT pathway in vivo. Gene Expr. Patterns *7*, 323–331.

Buch, S., Melcher, C., Bauer, M., Katzenberger, J., and Pankratz, M.J. (2008). Opposing effects of dietary protein and sugar regulate a transcriptional target of *Drosophila* insulin-like peptide signaling. Cell Metab. *7*, 321–332.

Colombani, J., Raisin, S., Pantalacci, S., Radimerski, T., Montagne, J., and Léopold, P. (2003). A nutrient sensor mechanism controls *Drosophila* growth. Cell *114*, 739–749.

Enell, L.E., Kapan, N., Söderberg, J.A., Kahsai, L., and Nässel, D.R. (2010). Insulin signaling, lifespan and stress resistance are modulated by metabotropic GABA receptors on insulin producing cells in the brain of *Drosophila*. PLoS One *5*, e15780.

Fei, H., Chow, D.M., Chen, A., Romero-Calderón, R., Ong, W.S., Ackerson, L.C., Maidment, N.T., Simpson, J.H., Frye, M.A., and Krantz, D.E. (2010). Mutation of the *Drosophila* vesicular GABA transporter disrupts visual figure detection. J. Exp. Biol. *213*, 1717–1730.

Géminard, C., Rulifson, E.J., and Léopold, P. (2009). Remote control of insulin secretion by fat cells in *Drosophila*. Cell Metab. *10*, 199–207.

Georgel, P., Naitza, S., Kappler, C., Ferrandon, D., Zachary, D., Swimmer, C., Kopczynski, C., Duyk, G., Reichhart, J.M., and Hoffmann, J.A. (2001). *Drosophila* immune deficiency (IMD) is a death domain protein that activates antibacterial defense and can promote apoptosis. Dev. Cell *1*, 503–514.

Gutierrez, E., Wiggins, D., Fielding, B., and Gould, A.P. (2007). Specialized hepatocyte-like cells regulate *Drosophila* lipid metabolism. Nature *445*, 275–280.

Halter, D.A., Urban, J., Rickert, C., Ner, S.S., Ito, K., Travers, A.A., and Technau, G.M. (1995). The homeobox gene repo is required for the differentiation and maintenance of glia function in the embryonic nervous system of *Drosophila melanogaster*. Development *121*, 317–332.

Hennig, K.M., Colombani, J., and Neufeld, T.P. (2006). TOR coordinates bulk and targeted endocytosis in the *Drosophila melanogaster* fat body to regulate cell growth. J. Cell Biol. *173*, 963–974.

Hombría, J.C., Brown, S., Häder, S., and Zeidler, M.P. (2005). Characterisation of Upd2, a *Drosophila* JAK/STAT pathway ligand. Dev. Biol. *288*, 420–433.

Ja, W.W., Carvalho, G.B., Mak, E.M., de la Rosa, N.N., Fang, A.Y., Liong, J.C., Brummel, T., and Benzer, S. (2007). Prandiology of *Drosophila* and the CAFE assay. Proc. Natl. Acad. Sci. USA *104*, 8253–8256.

Klagges, B.R., Heimbeck, G., Godenschwege, T.A., Hofbauer, A., Pflugfelder, G.O., Reifegerste, R., Reisch, D., Schaupp, M., Buchner, S., and Buchner, E. (1996). Invertebrate synapsins: a single gene codes for several isoforms in *Drosophila*. J. Neurosci. *16*, 3154–3165.

Luan, H., Lemon, W.C., Peabody, N.C., Pohl, J.B., Zelensky, P.K., Wang, D., Nitabach, M.N., Holmes, T.C., and White, B.H. (2006). Functional dissection of a neuronal network required for cuticle tanning and wing expansion in *Drosophila*. J. Neurosci. *26*, 573–584.

Mandal, L., Martinez-Agosto, J.A., Evans, C.J., Hartenstein, V., and Banerjee, U. (2007). A Hedgehog- and Antennapedia-dependent niche maintains *Drosophila* haematopoietic precursors. Nature *446*, 320–324.

Ni, J.Q., Markstein, M., Binari, R., Pfeiffer, B., Liu, L.P., Villalta, C., Booker, M., Perkins, L., and Perrimon, N. (2008). Vector and parameters for targeted transgenic RNA interference in *Drosophila melanogaster*. Nat. Methods *5*, 49–51.

Nicolaï, L.J., Ramaekers, A., Raemaekers, T., Drozdzecki, A., Mauss, A.S., Yan, J., Landgraf, M., Annaert, W., and Hassan, B.A. (2010). Genetically encoded dendritic marker sheds light on neuronal connectivity in *Drosophila*. Proc. Natl. Acad. Sci. USA *107*, 20553–20558.

O'Neill, E.M., Rebay, I., Tjian, R., and Rubin, G.M. (1994). The activities of two Ets-related transcription factors required for *Drosophila* eye development are modulated by the Ras/MAPK pathway. Cell *78*, 137–147.

Palanker, L., Tennessen, J.M., Lam, G., and Thummel, C.S. (2009). *Drosophila* HNF4 regulates lipid mobilization and beta-oxidation. Cell Metab. *9*, 228–239.

Pfeiffer, B.D., Ngo, T.T., Hibbard, K.L., Murphy, C., Jenett, A., Truman, J.W., and Rubin, G.M. (2010). Refinement of tools for targeted gene expression in *Drosophila*. Genetics *186*, 735–755.

Ranganayakulu, G., Schulz, R.A., and Olson, E.N. (1996). Wingless signaling induces nautilus expression in the ventral mesoderm of the *Drosophila* embryo. Dev. Biol. *176*, 143–148.

Slaidina, M., Delanoue, R., Gronke, S., Partridge, L., and Léopold, P. (2009). A *Drosophila* insulin-like peptide promotes growth during nonfeeding states. Dev. Cell *17*, 874–884.

White, B.H., Osterwalder, T.P., Yoon, K.S., Joiner, W.J., Whim, M.D., Kaczmarek, L.K., and Keshishian, H. (2001). Targeted attenuation of electrical activity in *Drosophila* using a genetically modified K(+) channel. Neuron *31*, 699–711.

Wu, Q., Zhang, Y., Xu, J., and Shen, P. (2005). Regulation of hunger-driven behaviors by neural ribosomal S6 kinase in *Drosophila*. Proc. Natl. Acad. Sci. USA *102*, 13289–13294.

Xu, K., Zheng, X., and Sehgal, A. (2008). Regulation of feeding and metabolism by neuronal and peripheral clocks in *Drosophila*. Cell Metab. *8*, 289–300.

Zinke, I., Kirchner, C., Chao, L.C., Tetzlaff, M.T., and Pankratz, M.J. (1999). Suppression of food intake and growth by amino acids in *Drosophila*: the role of pumpless, a fat body expressed gene with homology to vertebrate glycine cleavage system. Development *126*, 5275–5284.

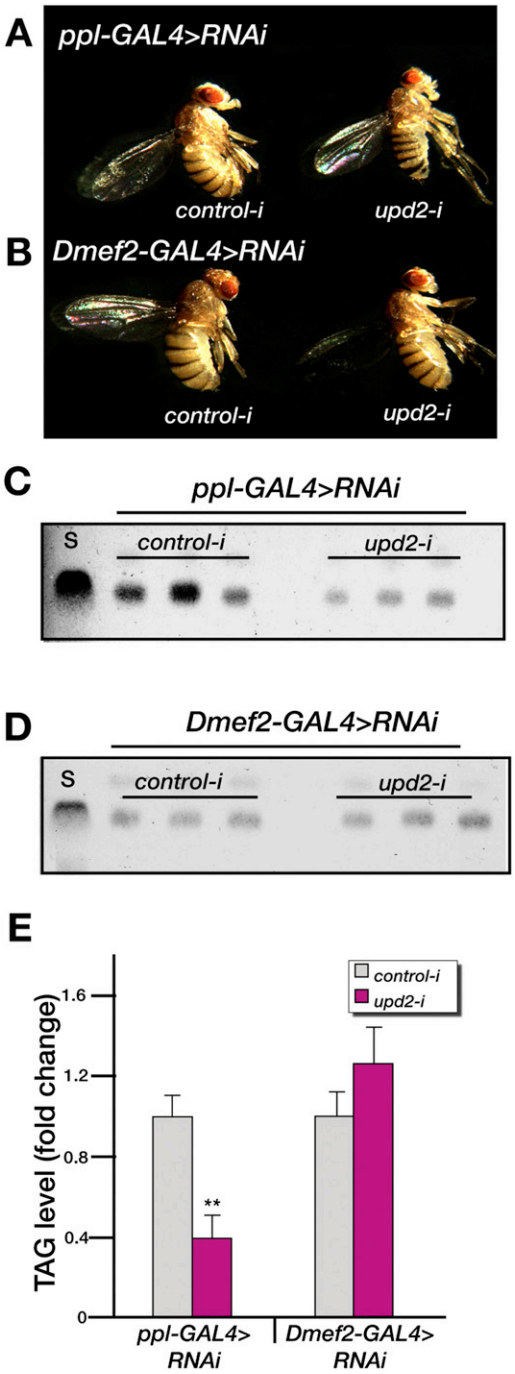

Figure S1. Upd2 Plays an FB-Specific Role in Regulating Systemic Growth and Metabolism, Related to Figure 1

(A and B) Adult female flies with FB-specific (A) and muscle-specific (B) knockdown of *upd2*. Only an *upd2* FB-specific knockdown results in growth defects (A). (C–E) TLC done on adult male flies that harbor an FB-specific (C) or muscle-specific (D) knockdown of *upd2*. Compromising *upd2* function in the FB results in reduced stored fat (C and E), whereas knocking it down in the muscle has no effect on fat storage (D and E). *control-i* refers to *GFP-RNAi*, and the *upd2(NP)-RNAi* line was used to knock down *upd2* in these experiments (*upd2-i*). The p values were calculated using Welch's t test; $^{**}p < 0.001$. S in TLC refers to the coconut oil standard in the TLC assay. Error bars indicate the SD.

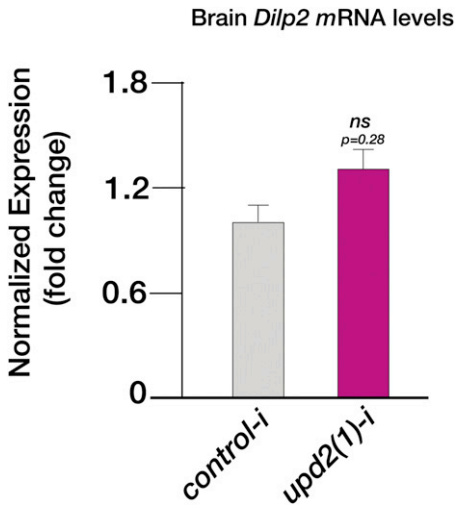

Figure S2. Dilp2 mRNA Levels in the Brain Are Not Significantly Altered in Flies with FB-Specific *upd2* RNAi, Related to Figure 3

Total RNA was extracted from brains of male larvae (see Extended Experimental Procedures), and the expression of *Dilp2* was analyzed by qPCR. The level of *Dilp2* mRNA in the brain is not significantly altered when *upd2* is knocked down in the FB. The p values were calculated using Welch's t test. Error bars indicate the SD.

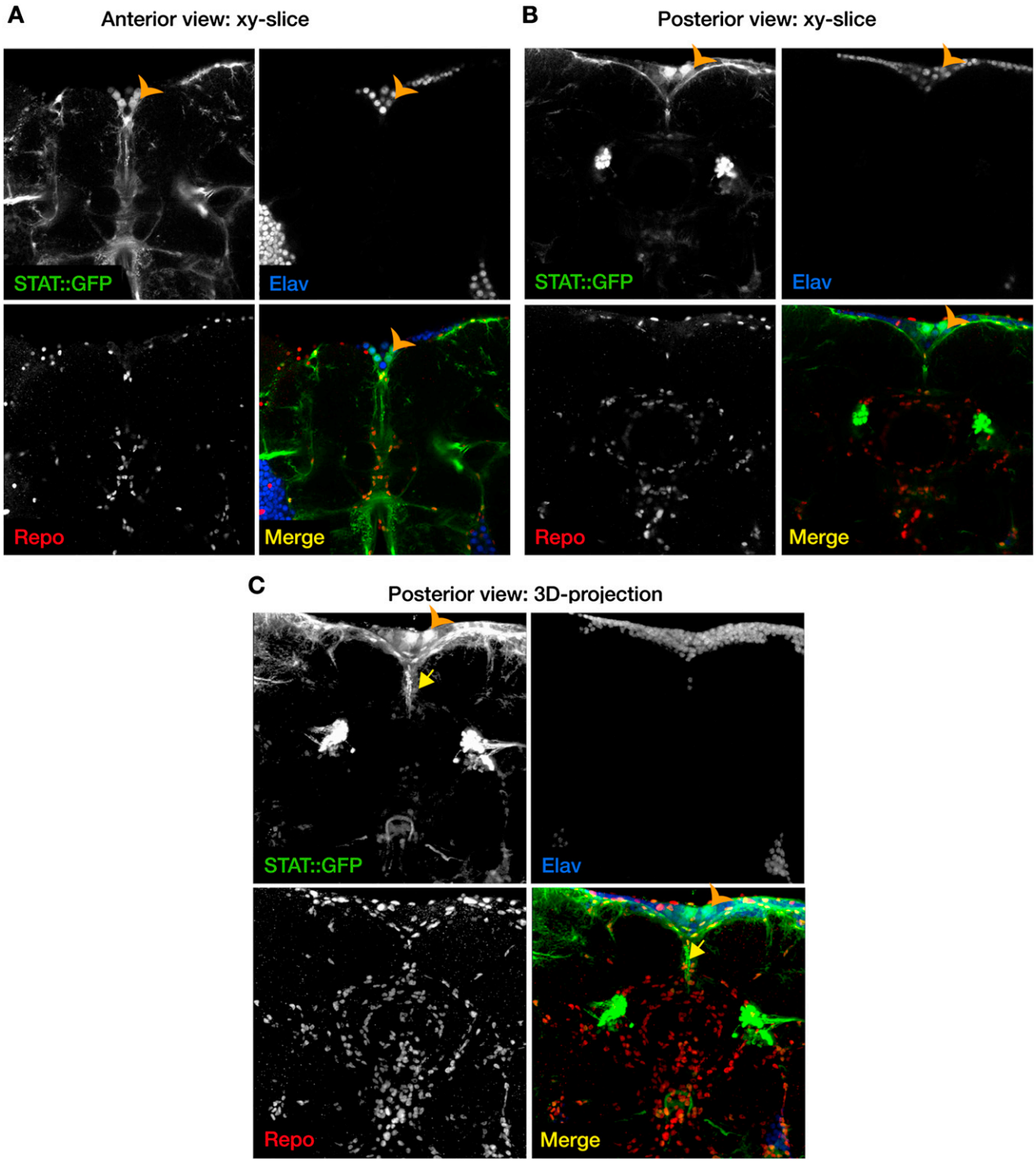

Figure S3. STAT::GFP Reporter Cells in the mNSC Region Are Expressed in Neurons, Related to Figure 4

(A–C) Single XY confocal sections of anterior (A), posterior (B), and three-dimensional XY projection (C) of adult male brains expressing the STAT::GFP reporter (green) immunostained with Elav, a neuronal nuclear marker (blue), and Repo, which is expressed in the glial cell nucleus (red). The STAT reporter expressing cells in the median neurosecretory region colocalize with the neuronal marker (orange arrowhead). The yellow arrow points to the bouton-like structure described in the Results section.

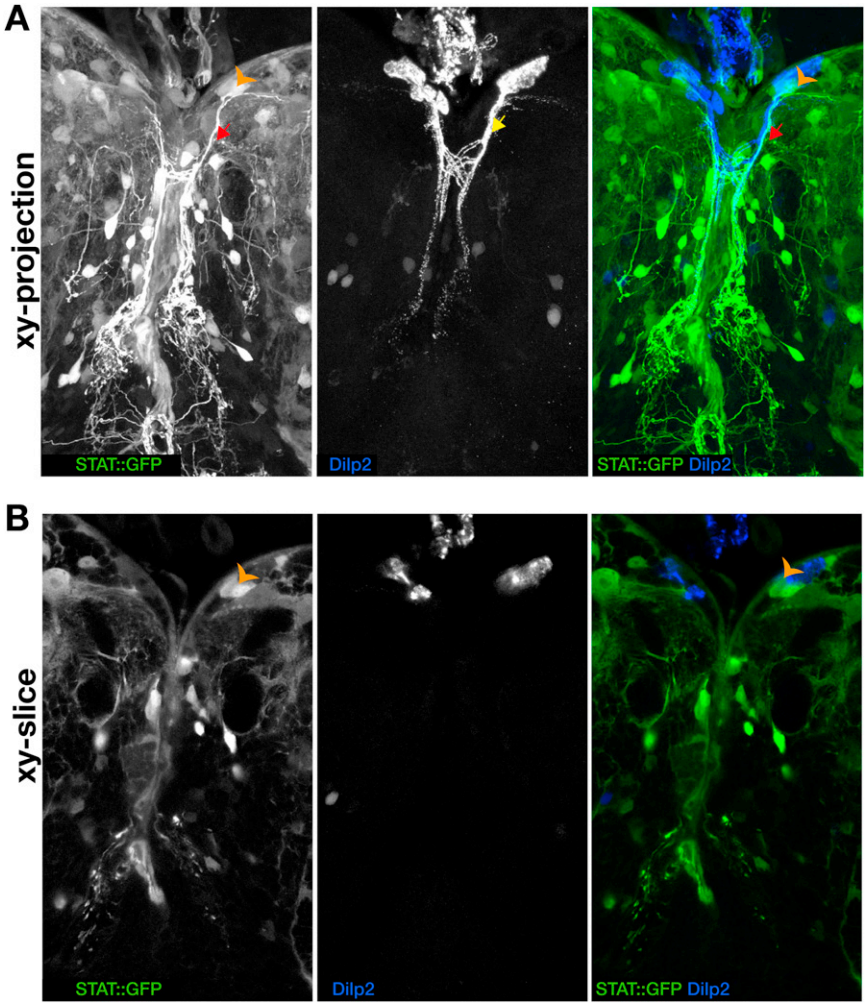

Figure S4. STAT::GFP Reporter Is Expressed in Neurons Juxtaposed with Dilp2-Producing IPCs in the Larval Brain, Related to Figure 4
(A and B) An XY projection (A) and a single confocal section (B) of larval brains expressing STAT::GFP reporter (green) immunostained for Dilp2 (blue). The STAT reporter is expressed widely, and is expressed in cells juxtaposed with Dilp-producing IPCs (orange arrowhead). The red arrow in A points to processes from the STAT reporter neurons, which run adjacent to the Dilp2 neurons.

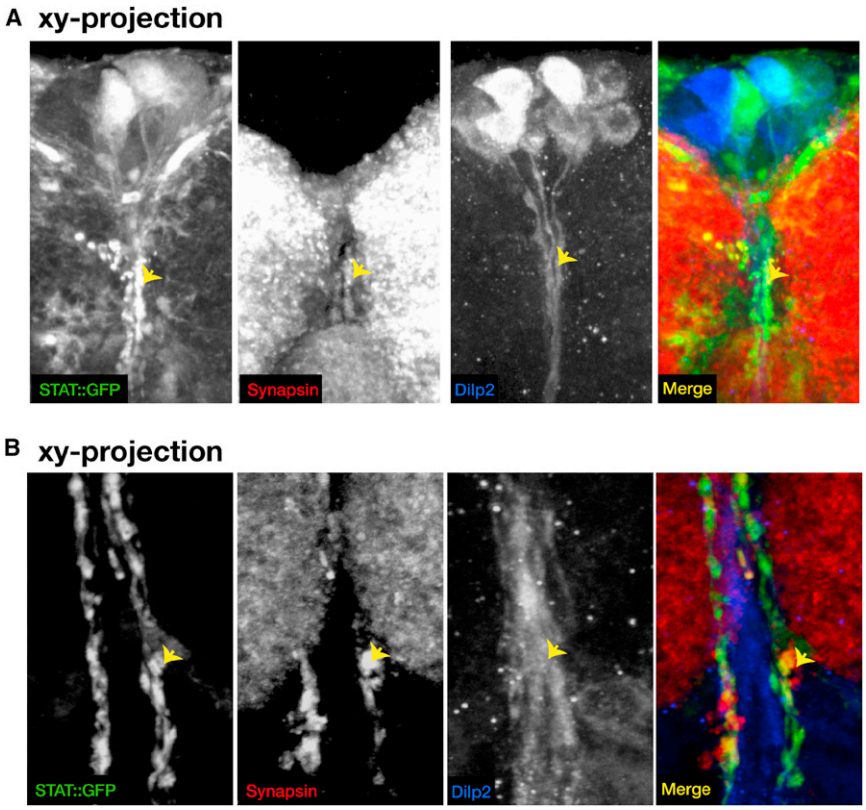

Figure S5. A Presynaptic Marker Is Colocalized with Bouton-Like Structures of the STAT::GFP Reporter, Related to Figure 4

(A and B) Images show XY projections of a few confocal slices at lower (40×, A) and higher (63×, B) magnification. Synapsin (red) is a presynaptic marker that localizes to synaptic junctions. The bouton-like structure of the STAT reporter neurons (green), which are adjacent to the Dilp2-expressing processes (blue), colocalize with synapsin (yellow arrows).

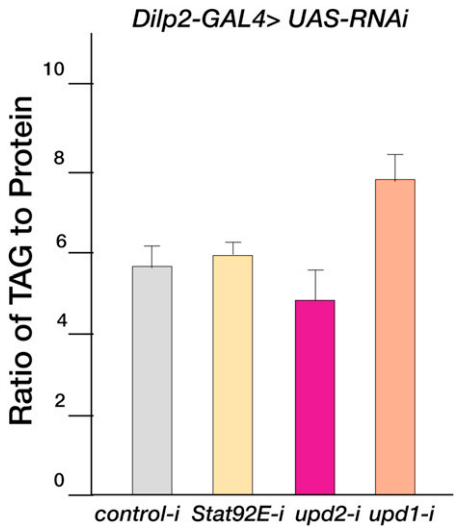

Figure S6. TAG Levels Are Unaltered when JAK/STAT Components Are Knocked Down in Dilp Neurons, Related to Figure 6

Quantification of the ratio of TAG to protein in adult males with IPC-specific knockdown of JAK/STAT pathway components. Results from two independent experiments are represented. No significant change in TAG levels is observed. *control-i* refers to *Luciferase-RNAi*. Error bars represent the SD.

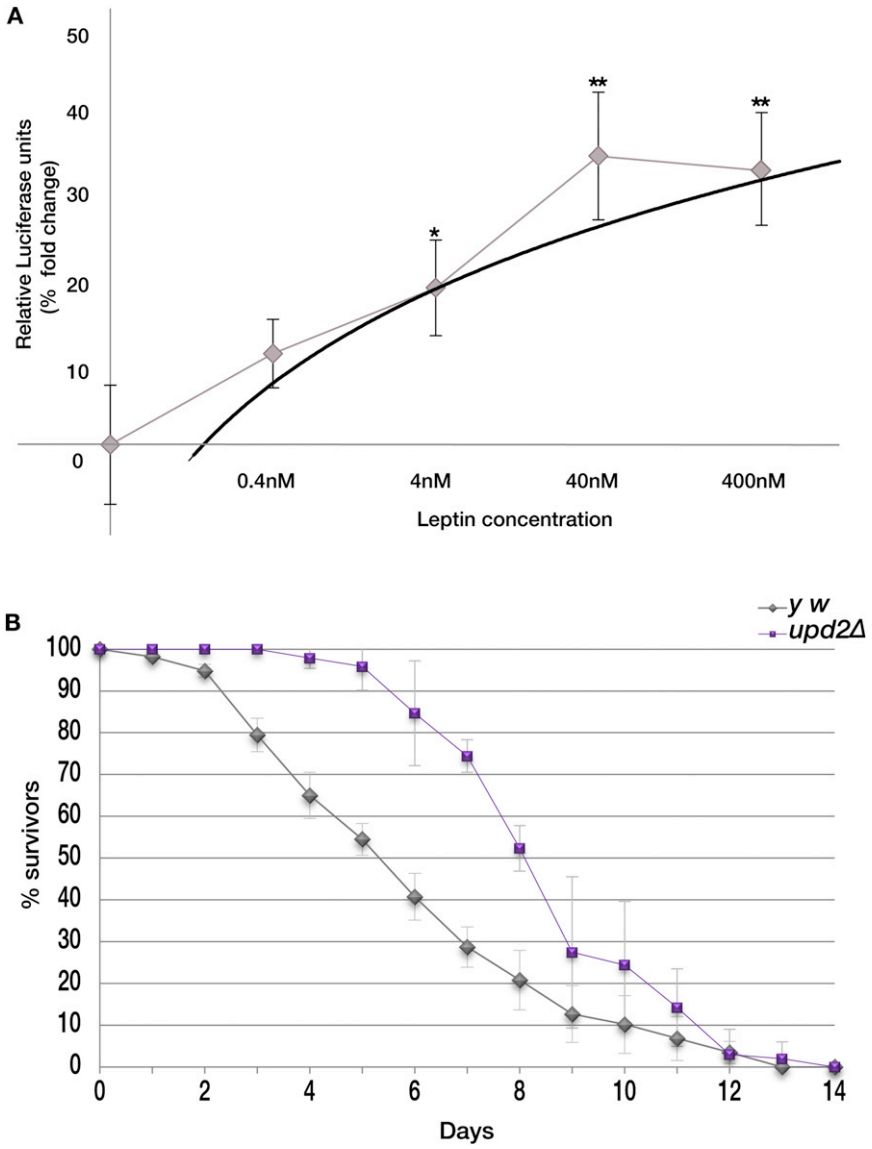

Figure S7. Human Leptin Can Signal through the *Drosophila* JAK/STAT Receptor and Upd2 Plays a Role Physiologically Similar to that of Leptin during Starvation, Related to Figure 7

(A) Affinity of human Leptin for the Dome receptor. Luciferase activity was measured after 30 hr of activation with Leptin at different concentrations. The Michaelis constant, K_m (the concentration of the substrate at which the reaction rate is half-maximum), is equal to 2.37 nM. The experiment was done in six biological replicates. *$p < 0.1$;**$p < 0.001$; p values were calculated using Welch's t test. Error bars indicate percent SD.

(B) *upd2Δ* adults are resistant to starvation. Survival of 10-day-old adult males on 1% sucrose agar at 25°C, n = 60 for *upd2Δ* (triplicates of n = 20), n = 80 for *y w* (four replicates of n = 20). Error bars represent SD.